

# Newcastle University e-prints

---

**Date deposited:** 18th August 2010

**Version of file:** Author, final

**Peer Review Status:** Peer reviewed

## Citation for published item:

Proctor CJ, Lydall D, Boys RJ, Gillespie CS, Shanley D, Wilkinson DJ, Kirkwood TBL. [Modelling the checkpoint response to telomere uncapping in budding yeast](#). *Journal of the Royal Society Interface* 2007,4 12 73-90.

## Further information on publisher website:

<http://royalsociety.org/>

## Publishers copyright statement:

This paper originally published by The Royal Society, 2007 and available (with permissions) from the URL below:

<http://dx.doi.org/10.1098/rsif.2006.0148>

Always use the published version when citing.

## Use Policy:

The full-text may be used and/or reproduced and given to third parties in any format or medium, without prior permission or charge, for personal research or study, educational, or not for profit purposes provided that:

- A full bibliographic reference is made to the original source
- A link is made to the metadata record in Newcastle E-prints
- The full text is not changed in any way.

The full-text must not be sold in any format or medium without the formal permission of the copyright holders.

**Robinson Library, University of Newcastle upon Tyne, Newcastle upon Tyne.**

**NE1 7RU.**

**Tel. 0191 222 6000**

## **Modelling the checkpoint response to telomere uncapping in budding yeast**

C.J. Proctor<sup>1,3</sup>, D.A. Lydall<sup>1,3</sup>, R.J. Boys<sup>2,3</sup>, C.S. Gillespie<sup>2,3</sup>, D.P. Shanley<sup>1,3</sup>, D.J.  
Wilkinson<sup>2,3</sup>, T.B.L. Kirkwood<sup>1,3</sup>

<sup>1</sup>*Institute for Ageing and Health, and School of Clinical Medical Sciences-  
Gerontology, Newcastle University, UK*

<sup>2</sup>*School of Mathematics & Statistics, Newcastle University, UK*

<sup>3</sup>*Centre for Integrated Systems Biology of Ageing and Nutrition, Newcastle  
University, UK*

## Abstract

One of the DNA-damage response mechanisms in budding yeast is temporary cell cycle arrest while DNA repair takes place. The DNA-damage response requires the co-ordinated interaction between DNA repair and checkpoint pathways. Telomeres of budding yeast are capped by the Cdc13 complex. In the temperature-sensitive *cdc13-1* strain, telomeres are unprotected over a specific temperature range leading to activation of the DNA-damage response and subsequently cell cycle arrest.

Inactivation of *cdc13-1* results in the generation of long regions of single-stranded DNA and is affected by the activity of various checkpoint proteins and nucleases.

This paper describes a mathematical model of how uncapped telomeres in budding yeast initiate the checkpoint pathway leading to cell cycle arrest. The model was encoded in the Systems Biology Mark-up Language (SBML) and simulated using the stochastic simulation system BASIS (**B**iology of **A**geing e-**S**cience **I**ntegration and **S**imulation). Each simulation follows the time course of one mother cell keeping track of the number of cell divisions, the level of activity of each of the checkpoint proteins, the activity of nucleases and the amount of single-stranded DNA generated. The model can be used to carry out a variety of “*in silico*” experiments in which different genes are knocked out and the results of the simulation are compared to experimental data. Possible extensions to the model are also discussed.

Keywords: systems biology, modelling, stochastic, telomere, checkpoint, yeast,  
CDC13

## 1. Introduction

Telomeres are repetitive sequences of DNA situated at the ends of linear chromosomes. They require protection from being recognised as double strand breaks to prevent activation of the DNA-damage response. In budding yeast, the telomere-binding protein Cdc13 provides a protective cap at the ends. In the absence of Cdc13, checkpoint proteins bind to the telomeres, resulting in cell cycle arrest (Weinert & Hartwell, 1988; Lydall, 2003), accumulation of single-stranded DNA on the 3' strands (Garvik et al., 1995) and recombination (Grandin et al., 2001a). A mutant form of Cdc13, *cdc13-1*, has a temperature dependant response and is only able to cap telomeres at a range of temperatures, with the maximum “permissive temperature” being 25°C (Garvik et al., 1995). At higher temperatures, *cdc13-1* is unable to function, the checkpoint pathway is activated and the cells stop growing. So a temperature in this range is referred to as a “restrictive temperature”. A useful way to study the checkpoint response in budding yeast is to introduce the *cdc13-1* mutation and to initially culture the cells at a permissive temperature (e.g. 23°C) and then switch to a restrictive temperature (e.g. 36°C). Throughout this paper we will use the terms “permissive temperature” and “restrictive temperature” to refer to *cdc13-1* strains being cultured at 23°C and 36°C respectively. More detail of the experimental framework can be found in Zubko et al. (2004).

The end of a telomere in budding yeast consists of a very short region of single-stranded DNA (about 12 nt) which is termed an “overhang” (Larrivee et al., 2004). This overhang is usually protected by telomere-binding proteins to prevent it from being seen as DNA damage, which would otherwise activate a DNA damage response. At the restrictive temperature *cdc13-1* cells possess a small amount of

DNA-damage, as a result of overhangs becoming exposed, that activates the Rad9- and Rad24-dependent checkpoint pathway. This initial damage is amplified to larger single-stranded regions near telomeres. The generation of single-stranded DNA is a necessary requirement for the full activation of the checkpoint response. There is evidence that the Mrx complex, Exo1 and the Rad24 group regulate or encode nucleases which are responsible for generating single-stranded DNA (ssDNA) at telomeres (Lydall, 2003). Exo1 regulates ssDNA levels when telomere capping is defective. For example, Exo1 is essential for ssDNA generation in *yku70Δ* mutants and contributes to ssDNA in *cdc13-1* mutants (Maringele & Lydall, 2002). In *cdc13-1rad9Δ* mutants the ssDNA accumulates more rapidly than in *cdc13-1* mutants, but in *cdc13-1rad24Δ* mutants the ssDNA accumulates much more slowly than in *cdc13-1* cells (Lydall & Weinert, 1995). It has been found that ssDNA levels are high in *cdc13-1 rad9Δ exo1Δ* strains, low in *cdc13-1 exo1Δ* strains, and low in *cdc13-1 rad53Δ exo1Δ* and *cdc13-1 mec1Δ exo1Δ* strains (Jia et al., 2004; Zubko et al., 2004). This suggests that Rad9 inhibits an unidentified nuclease called ExoX, and that this inhibition does not require Mec1 or Rad53.

In order to understand precisely how this important yet complex system of pathways is regulated, there is a clear role for mathematical models. These can help both to reveal gaps and inconsistencies in current knowledge and also to conduct *in silico* experiments (simulations) that can help in the efficient planning of wet experimental studies. A model for the interaction of checkpoint pathways and nucleases at *cdc13-1* induced damage has been proposed by Jia et al. (2004). The model from their paper has been reproduced in figure 1. The Rad17, Mec3, and Dcd1 complex is a heterotrimeric PCNA-type ring which is loaded onto damaged telomeres by another

complex consisting of Rad24 and Rfc2-5 subunits, which together form a clamp-clamp loader system (Majka & Burgers, 2003). Once loaded the Rad17 complex activates ExoX. ExoX generates single-stranded DNA at the telomeres. Mec1 and Ddc2 bind single-stranded DNA independently of the Rad17 complex. Mec1 is essential for phosphorylation and activation of Rad9, which in turn activates two parallel pathways of cell cycle arrest. One pathway is via the kinase Chk1 and the other pathway is via the kinase Rad53 (Gardner et al., 1999, Sanchez et al., 1999). Rad9 also inhibits the activity of ExoX (Zubko et al., 2004). Exo1 activity is not dependent on Rad24 or Rad17 but its activity is inhibited by Rad53. It has been proposed that Rad9 mediates interactions between the upstream kinase Mec1 and two parallel downstream kinases Rad53 and Chk1 (Blankley & Lydall, 2004, Gilbert et al., 2001, Schwartz et al., 2002).

In a study of yeast checkpoint genes, it was found that there was a correlation between the amount of ssDNA and cell death in several single and double mutant strains (Lydall & Weinert, 1995). However, more recently it has been found that *mec1Δ*, *rad53Δ* and *exo1Δ* mutations each suppress the rapid loss in viability of *cdc13-1 rad9Δ* mutants but ssDNA still accumulates (Jia et al., 2004). They suggest that ssDNA is only cytotoxic if Mec1, Rad53 and Exo1 convert it into a lethal lesion.

The biochemical mechanisms underlying the DNA-damage response are complex and many hypotheses have been put forward to suggest how DNA repair and checkpoint pathways interact. This has motivated us to develop a mathematical model of the system. To build the model it was necessary to specify precisely each element of the network and its interaction with other elements (see Section 2.1 for details).

## **2. The Model**

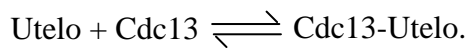
### **2.1. Elements of the Model**

The paper describes a core model representing the wild type from which a number of variants were created to represent a number of experimental knockouts. The set of models all contain the same network but the variants have different sets of parameter values or initial conditions (see table 3). The differences are typically small but lead to significant variance in phenotype. We use the term “species” to denote a biochemical entity in the model and interactions between species are referred to as reactions. These terms will be used throughout this paper. The first step in building the model is to define all the species and to specify their initial amounts. A complete list for the wild type variant is given in table 1 and each of the species and all the reactions in the model are described in detail below. A complete list of the reactions and their parameters (for the wild type variant) is given in table 2. We use mass action stochastic kinetics for the rate laws (see Wilkinson (2006) for further details). We also use event structures in our model which allows species amounts and parameter values to be changed once a particular condition is true. These are detailed in the text and summarised in table 3. Figure 2 contains a diagram of the reaction network in the model.

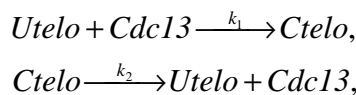
#### **2.1.1 Capped telomeres, uncapped telomeres and Cdc13**

Budding yeast have 16 chromosomes and hence 32 telomeres in G1 but during S phase, the DNA is replicated resulting in 64 telomeres. To avoid unnecessary complexity, we have omitted detail of DNA replication from this model and assumed that the number of telomeres is constant. The main purpose of this model is to examine the pathways that lead to G2/M arrest and so we have chosen 64 telomeres.

Telomeres can be in either a capped or uncapped state and so we have two species to represent telomeres which we call Utelo and Ctelo for uncapped and capped telomeres respectively. We assume that the ssDNA overhangs at the telomere ends are capped by Cdc13. The dissociation rate (the time required for half the protein-DNA complex to dissociate) is approximately 30 minutes (Lin et al., 2001). Cdc13 has a strong binding affinity to single-stranded telomeric DNA with a dissociation constant of about  $10^{-7}$  M (Lin et al., 2001). So there is equilibrium between uncapped telomeres (Utelo) and those bound by Cdc13:



To model this equilibrium we set up two reactions:



where Ctelo represents the pool of telomeres bound by Cdc13.

The first reaction represents capping and the second reaction uncapping. The capping reaction is a second-order reaction since there are two reactants and is given by

$k_1[\#\text{Utelo}][\#\text{Cdc13}]$ , where # represents the number of molecules. The uncapping

reaction is a first-order reaction and is given by  $k_2[\#\text{Ctelo}]$ . The value of  $k_2$  can be

calculated using information on the time taken for half of the bound Cdc13 to

dissociate from the telomere given above. Since the biological half-life is given by  $t_{1/2}$

$= -\ln(0.5)/\text{degradation rate}$ , it follows that  $k_2 = -\frac{\ln(0.5)}{30 \times 60} \text{ s}^{-1} = 3.85 \times 10^{-4} \text{ s}^{-1}$ . The dissociation

constant  $k_d$  is  $10^{-7}$  M = 110 molecules/nucleus, assuming that the volume of a yeast

nucleus is about  $1.8 \mu\text{m}^3$  ( $1.8 \times 10^{-9}$   $\mu\text{litres}$ ) ([http://biochemie.web.med.uni-](http://biochemie.web.med.uni-muenchen.de/Yeast_Biol/)

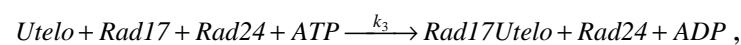
[muenchen.de/Yeast\\_Biol/](http://biochemie.web.med.uni-muenchen.de/Yeast_Biol/)). Since  $k_d = k_2 / k_1$ , then  $k_1 = 3.6 \times 10^{-6} \text{ molecule}^{-1} \text{ s}^{-1}$ . We

assume that all telomeres are in a capped state initially but there is a dynamic process

of uncapping and recapping so that at any point in time there is a very low number of uncapped telomeres. Telomeres remain in an uncapped state only very transiently, and signalling proteins do not bind while they are in this transient state.

### 2.1.2 Binding of uncapped telomeres: Rad17 and Rad24

If a telomere remains uncapped, then the Rad17 complex is loaded onto the telomere end by the Rad24 clamp loader complex. This loading requires ATP and can be represented by the biochemical reaction:



where *Rad17Utelo* represents the binding of Rad17 to the telomere end. For simplicity we have omitted details of Mec3 and Ddc1 in the Rad17 complex and omitted the Rfc2-5 subunits in the Rad24 complex, since they are unimportant for this model. Since there are four reactants in the Rad17-binding reaction, the stochastic rate law is a fourth-order reaction. Care needs to be taken when considering higher-order reactions. For example it is not realistic that the reaction rate would increase indefinitely with an increase in ATP levels; doubling the level of ATP in the cell would not necessarily double the reaction rate. Instead we would expect that the reaction rate would increase asymptotically with ATP levels. Therefore we use the rate law  $k_3[\#Utelo][\#Rad17][\#Rad24][\#ATP]/(5000+[\#ATP])$ .

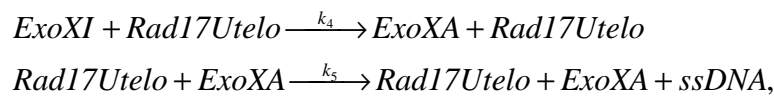
The term in the denominator ensures that the reaction rate increases approximately linearly with ATP when ATP levels are low (less than about 2000) but for high levels of ATP (greater than 5000) the increase in the reaction rate starts to level off with increasing ATP levels. The value for  $k_3$  was chosen by making an initial estimate and then simulating the model and comparing the model output to experimental data.

Further details of how we chose parameter values can be found in section 2.3.

When Cdc13 is present, this reaction is very unlikely to occur as the binding strength of Rad17 compared to Cdc13 is extremely low. However, in the absence of Cdc13, this reaction will eventually take place and an irreversible set of reactions is initiated leading to the generation of ssDNA and cell cycle arrest unless the pathway is interrupted downstream. We chose a very low value for  $k_3$ , to ensure that the probability of a telomere, which is only transiently uncapped, binding to Rad17 is very low.

### 2.1.3. Nuclease activity: ExoX, Exo1 and ssDNA

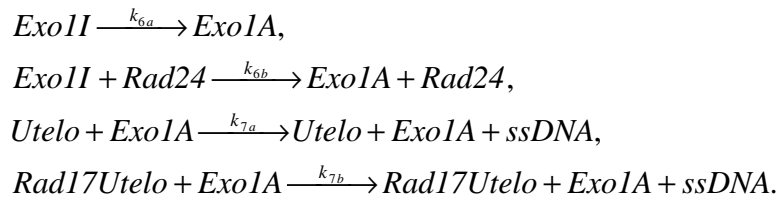
ExoX is recruited to telomeres bound by Rad17, and degrades one of the strands to leave a long stretch of single-stranded DNA. This reaction can only occur if ExoX is in its active state. The binding of telomeres by Rad17 (which in turn requires Rad24) is required for ExoX activation. This can be represented simply by the following reactions:



where ExoXI represents the inactive form of ExoX and ExoXA represents activated ExoX. We assume that each time this reaction takes place, 10nt of ssDNA are produced and we set one unit of ssDNA equal to 10nt. The reaction can continue to take place until ExoX is inactivated. It has been observed that about 8kb of ssDNA are generated in one hour in *cdc13-1* strains (Jia et al., 2004; Zubko et al., 2004).

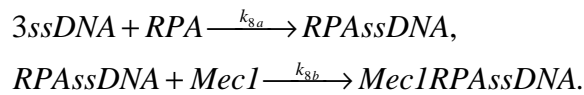
Exo1 degrades unprotected telomeres, independently of ExoX and Rad17, but also degrades telomeres bound by Rad17. Exo1 activation does not require Rad24. Since *cdc13-1 rad24Δ* mutants have low levels of single-stranded DNA (Lydall & Weinert, 1995), we assume that activation of Exo1 is much lower than the activation of ExoX. There are very low levels of single-stranded DNA in the *cdc13-1rad24Δ* strain, which

must be due to Rad24-independent activation and subsequent activity of Exo1. However the difference between the amounts of single-stranded DNA in *cdc13-1exo1Δ* compared to *cdc13-1* mutants is large (Zubko et al. 2004), suggesting that Exo1 is higher when Rad24 is present. Therefore we also include an additional reaction of Rad24 dependent activation of Exo1. The reactions for nuclease activity are below:



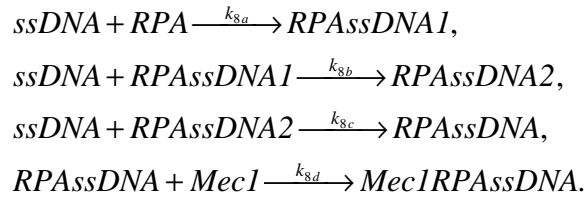
#### 2.1.4 Binding of ssDNA: RPA and Mec1

Replication protein A (RPA) binds to single-stranded DNA with every molecule of RPA binding to 30nt of ssDNA (Zou & Elledge, 2003). As each unit of ssDNA is equivalent to 10nt, we assume that one molecule of RPA binds to three units of ssDNA. Mec1 in complex with Ddc2 then binds to RPA (Zou & Elledge, 2003). So binding of ssDNA can be represented by the following two reactions:



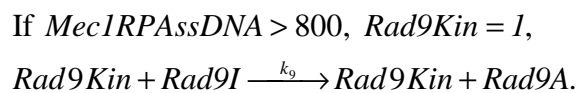
Since three units of ssDNA are required for the RPA binding reaction, the mass action stochastic kinetic rate law is given by  $k_{8a}[\#RPA][\#ssDNA][\#ssDNA-1][\#ssDNA-2]/6$ . However this rate law is only valid if the ssDNA units are independent. This is certainly not the case, and the rate law should be a linear and not a cubic function of the total amount of ssDNA, Therefore we model RPA binding as a series of steps. To do this we introduce two dummy species RPA<sub>ssDNA1</sub> and RPA<sub>ssDNA2</sub> for the intermediate steps. In the first step RPA binds to one unit of ssDNA to form RPA<sub>ssDNA1</sub>. The rate of this reaction depends linearly on the total amount of

ssDNA. In the next step, RPA<sub>ssDNA1</sub> binds to the second unit of ssDNA to form RPA<sub>ssDNA2</sub> and finally RPA<sub>ssDNA2</sub> binds to the third unit of ssDNA to form RPA<sub>ssDNA</sub>. Once the first step has happened, the next two steps follow quickly by setting the rate constants to a high value ( $k_{8b}=k_{8c}=100$ ). The full set of reactions for RPA and Mec1 binding are:

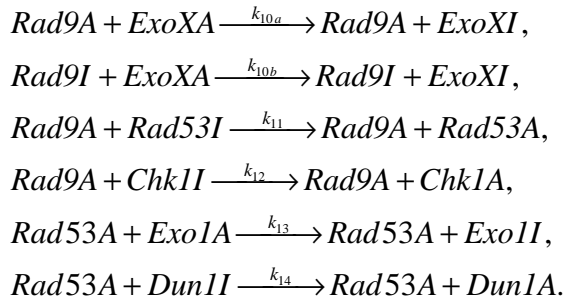


### 2.1.5. Checkpoint activation: Rad9, Rad53, Chk1 and Dun1

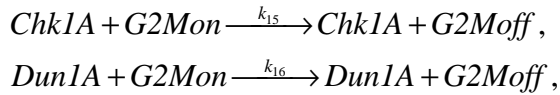
A very large threshold of about 10kb of single-stranded DNA is required for keeping checkpoints active in order to maintain cell cycle arrest (Vaze et al., 2002; Zubko et al., 2004; Maringele & Lydall, 2005). To prevent activation of Rad9 when only low levels of ssDNA are present we modelled this activation as a two-step process. First we used an event structure in the model to activate a kinase that activates Rad9 (called “Rad9Kin”) if the total amount of ssDNA within the cell exceeded 8kb. The rate for the Rad9-activation reaction is equal to  $k_9 [\#Rad9I][\#Rad9Kin]$  and will be equal to zero as long as Rad9Kin=0. Once Rad9Kin is activated (so that Rad9Kin=1), the Rad9-activation reaction can proceed. The event and reaction representing Rad9 activation are below:



Activated Rad9 activates both Rad53 and Chk1. Rad53 in turn, inhibits the activity of Exo1 and activates Dun1. Rad9 also inhibits ExoX. This inhibition does not require Rad9 to be activated by Mec1 and so is represented by two reactions, one with Rad9I and the other with Rad9A:



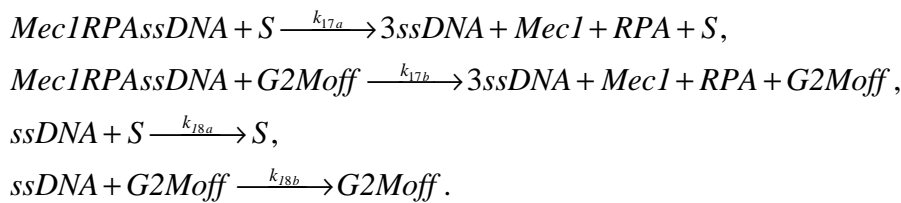
Activation of Chk1 and Dun1 results in G2/M arrest:



where  $G2Mon$  and  $G2Moff$  are dummy species which control whether the cell cycle can progress from G2 to M. If  $G2Mon=1$  and  $G2Moff=0$ , then the above reactions can occur. If  $G2Mon=0$  and  $G2Moff=1$ , then the reactions cannot take place. (See appendix 1 for details of modelling the cell cycle).

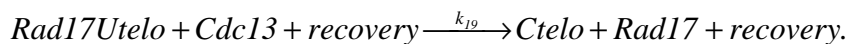
### 2.1.6 Recovery

Single-stranded DNA may be removed during S phase by DNA replication. It is also possible that ssDNA is removed during G2/M arrest. When all the ssDNA has been removed, the uncapped telomeres can be recapped by Cdc13 and recovery takes place. After recovery, all the checkpoint proteins are turned off and cell division can take place. This procedure is modelled by a series of reactions and events:



If  $Mec1RPA_{ssDNA} + RPA_{ssDNA} + ssDNA = 0$ , then  $recovery=1$  (where  $recovery$  is a dummy species in the model).

If  $recovery=1$ , then the following reaction can proceed:



If  $Rad17Utelo=0$  (i.e. all telomeres have been recapped), then  $G2Moff$  is set to zero,  $G2Mon$  is set to one,  $recovery$  is set to zero, and all other checkpoint proteins are reset to their initial conditions. A network diagram of the full system is shown in figure 2.

## 2.2 The cell cycle

We also include a series of reactions to represent the different stages of the cell cycle (see appendix 1). We assume that single stranded DNA can be removed by DNA replication when the cell is in S phase and also to a lesser extent when cells are in G2/M arrest. Although it is unclear whether DNA replication can take place in G2/M arrest, it has been observed that the level of ssDNA does decrease in cells which are arrested (Jia et al., 2004; Zubko et al., 2004). When budding yeast divide, the mother cell produces a small bud which then grows. When mitosis and cytokinesis is complete, the bud detaches to form the new daughter cell. This budding leaves a scar on the surface of the cell. Therefore, it is possible to count the number of cell divisions that a particular yeast cell has undergone by counting the number of budscars. We imitate this process in our model and keep track of the number of divisions by the introduction of a dummy species, *budscar*, which increases by one, every time the cell passes from the M phase to G1. The reaction and equation for the budscar species are shown in appendix 1.

## 2.3 Initial conditions and parameter values

Before a model can be simulated, the initial amount of each species must be specified. We obtained the majority of the initial amounts of proteins by consulting the yeast GFP fusion localisation database (<http://yeastgfp.ucsf.edu>; Huh et al., 2003). We

assume that initially all the checkpoint proteins are in their inactive state. In the G2 phase of the cell cycle, budding yeast contain 32 chromosomes and so have 64 telomeres which we assume are all initially bound by Cdc13. We do not include detail of DNA replication in our model and so assume that the total number of telomeres is constant. Table 1 lists all the species, their respective initial amounts, the systematic names of all genes and the database terms so that each entity can be identified in public accessible bioinformatics databases.

The rate constants for each of the reactions are listed in table 2. Note that the value of  $k_1$  was set at  $5 \times 10^{-4}$ , although we had calculated it to be  $3.6 \times 10^{-6}$  from published data (Lin et al., 2001), a hundred-fold difference. This is because with our original value of  $k_1$  we found that the binding of Cdc13 to telomeres was not strong enough to keep them in a capped state (see figure 3). Our model suggests that the binding of Cdc13 to telomeres must be stronger *in vivo* and it is probably the case that the binding affinity of Cdc13 is increased when it is in complex with Stn1 and Ten1 (Grandin et al., 2001b). At present there are no experimental data to support this but it seems a reasonable assumption. Therefore we increased the value of  $k_1$  until we obtained results in which telomeres only become uncapped transiently as in figure 3 and chose  $k_1 = 0.0005$  as our default value. Figure 4 shows the model predictions for the kinetics of uncapping for the *cdc13-1* strain when placed at the restrictive temperature using the default parameters. The only other kinetic data currently available for parameterising the model are rates of single strand production in *cdc13-1* mutants at high temperatures, where a rate of 8kb per hour has been observed (Jia et al., 2004; Zubko et al., 2004). The actual rates for the different nucleases are unknown but were

chosen to reflect the suggested relative difference and so we assumed that ExoX activity is ten times faster than ExoI activity.

We created an initial computer representation of the model using estimates for parameter values taken directly from evidence in the literature, where available. In some cases parameter values started as initial best guesses. This initial model was then simulated and the results compared to experimental data. Parameter values were then adjusted to ensure that the model complied with that data. We are confident that the adjustments we made to parameters were either to parameters for which we did not have specific data for or that the data was derived from in-vitro experiments which do not correspond to the in-vivo conditions of the culture experiments.

We coded the models in the Systems Biology Markup Language (SBML) Level 2 (Hucka et al., 2003). SBML is a way of representing biochemical networks and is now one of the standards used by the modelling community. It has been evolving since mid-2000 through the efforts of an international group of software developers and users. The models were developed using MathSBML (Shapiro et al., 2004). The final model for the wild type cell was encoded using SBML shorthand and then converted into full SBML (Wilkinson, 2006). The model was then imported into the BASIS system ([www.basis.ncl.ac.uk](http://www.basis.ncl.ac.uk)) and models for the mutant strains were created by making simple modifications to the original model.

To simulate the model we used a stochastic simulator based on the Gillespie algorithm (Gillespie 1977), since many of the processes being modelled occur at random times. This means that different outcomes may result from the same set of initial conditions.

Also some of the species in our model must be considered as discrete units rather than continuous variables. For example species representing the number of capped and uncapped telomeres must be a small integer and so it is not appropriate to use a deterministic simulator for this model. However, we also tried running simulations with a deterministic simulator to see if any parts of the model could be successfully modelled this way (see 3.3). Stochastic simulations were carried out on a Linux Beowulf cluster and the results are stored in a database. All the models and results in this paper are obtainable from the BASIS website ([www.basis.ncl.ac.uk](http://www.basis.ncl.ac.uk)). For further details see Gillespie et al. (2006a, 2006b). The model for the wild type strain, where cell death is included, is also available from the Biomodels database (ID:MODEL8679489165) at <http://www.ebi.ac.uk/biomodels/> (Le Novere et al., 2006).

We did not carry out a full sensitivity analysis for the model parameters as this would have been very time-consuming due to the number of parameters and the fact that we used a stochastic simulator. However, many of the model parameters were chosen after many trials with different values and so it is possible to discuss the effects of changing these. The checkpoint response is sensitive to changes by an order of magnitude to the values of the parameters for the rate of capping ( $k_1$ ) and Rad17 binding to uncapped telomeres ( $k_3$ ). A ten fold decrease in  $k_1$  or a ten fold increase in  $k_3$  lead to an over-activation of the checkpoint response. The parameters involved in nuclease activity and removal of single-stranded DNA were confined within fairly limited ranges in order to obtain rates of single-stranded DNA production observed in *cdc13-1* mutant strains. The parameters for cell cycle arrest ( $k_{15}$  and  $k_{16}$ ) could be increased with little effect on the model predictions but lowering the values led to an

unsustained cell cycle arrest which could easily be overcome by Cdk activity. The rate of Rad9 activation ( $k_9$ ) was the most important parameter in the checkpoint pathway and affected not only how quickly the cell responded once the threshold level of single-stranded DNA was reached but also how quickly nuclease activity was inhibited. The other parameters in the checkpoint response had no significant effect on the model predictions for the rate of ssDNA production or the number of divisions before cell cycle arrest or cell death. For example, a ten-fold increase or decrease on the rate of Mec1 binding (parameter  $k_{8d}$ ) did not change the rate of ssDNA production, the total level of ssDNA, or the number of divisions before cell cycle arrest.

### **3. Results**

#### **3.1. Wild-type cells**

The model predicts that capped telomeres may become transiently uncapped but are then recapped. At any one time, there is usually only one uncapped telomere at most but on occasion, two or three telomeres may be uncapped simultaneously (figure 3). However, they do not remain uncapped long enough for Rad17 to bind, so very little ssDNA is produced (data not shown). Figure 5 shows the model predictions for the number of divisions obtained in three different simulation runs. Since we have used a stochastic simulator, each run produces a slightly different output. The cells divide about 7-9 times in a period of 12 hours which gives an average division time of about 1.5 hours. This corresponds to the division time obtained when wild type cells are grown at the restrictive temperature.

#### **3.2. *Cdc13-1* mutant strains.**

##### **3.2.1. Cell divisions**

We used our model to simulate *cdc13-1* mutant strains at the restrictive temperature by setting the initial amount of *Cdc13*=0, *Ctelo*=0 and *Utelo*=64. We can also examine the effects of knocking out different genes for checkpoint proteins and nucleases. For example, to simulate a *cdc13-1rad9Δ strain*, we set the initial amount of *Rad9I*=0. Our model predicts that *cdc13-1* cells are unable to divide, although occasionally they may divide once before cell cycle arrest occurs (data not shown). This is due to the uncapped telomeres being bound by Rad17 which then initiates a series of events leading to cell cycle arrest. Both Rad9 and Rad24 are required for cell cycle arrest to occur. Our model predicts that *cdc13-1exo1Δ* double mutants enter cell cycle arrest after a few divisions as ssDNA can still be produced through the activity of ExoX and so Rad9 is activated and in turn the other checkpoint proteins are activated. The later activation of the checkpoint response is due to the slower generation of ssDNA without the activity of Exo1. Figure 6 shows data from Zubko et al. (2004) for various yeast strains cultured at the restrictive temperature. *cdc13-1* mutants are unable to divide at the restrictive temperature but knocking out Rad24, Rad9 or Exo1 restores cell division so that microcolonies form. Both *cdc13-1rad9Δ* and *cdc13-1exo1Δ* double mutants at the restrictive temperature have very small micro-colonies, although we would expect that knocking out Rad9 would prevent cell cycle arrest. The cells for *cdc13-1exo1Δ* strain are larger than in the *cdc13-1rad9Δ* strain which indicates that cells initially arrest and then eventually escape this arrest and divide a few times before cell death takes place. *cdc13-1* strains accumulate large amounts of ssDNA since nuclease activity is intact and this is probably the cause of cell death. If we compare the model output with experimental data, we see good agreement apart from the *cdc13-1rad9Δ* mutant. Our model predicts that *cdc13-1rad9Δ* cells keep dividing but experimental data show that these cells only form

very small micro-colonies (see figure 6). This is because we had not included the possibility of cell death in the model. To take cell death into account, we modified the model (see section 3.2.3). Our model also does not fit the observation of cell cycle arrest followed by escape for the *cdc13-1exo1Δ* strain as we have not included this mechanism in the model. We outline a possible extension to include this escape mechanism in the discussion section.

### **3.2.2. Generation of single-stranded DNA**

Zubko et al. (2004) showed that large amounts of single-stranded DNA are produced in *cdc13-1* mutants at the restrictive temperature, but that deleting Exo1 considerably reduced these levels. Deleting Rad24 also reduced the amount of single-stranded DNA but deleting Rad9 had the opposite effect (see Zubko et al., 2004). Therefore we plotted the level of single-stranded DNA at different time points for each of the different mutant strains and compared our results to Zubko et al.'s (2004) data.

Our models predict that initially large amounts of ssDNA are generated in *cdc13-1* strains (see figure 7) but this stabilizes when cells enter G2/M arrest, as nuclease activity is inhibited by Rad9 and Rad53. Large amounts of ssDNA are generated in *cdc13-1rad9Δ* double mutants since Rad9 is required to inhibit nuclease activity. In contrast, only small amounts of ssDNA are generated in *cdc13-1rad24Δ* double mutants. This is due to the fact that in our model Rad24 is required to load Rad17 onto uncapped telomeres and so activate ExoX. Our model predicts that much lower levels of ssDNA are generated in *cdc13-1exo1Δ* double mutants than in the *cdc13-1* strain. This low level of ssDNA is due to the residual activity of ExoX, which has not been completely inhibited by Rad9. The generation of ssDNA in the *cdc13-*

*1rad24* $\Delta$  strain is due to the Rad24-independent activity of Exo1 and the difference between the amount of ssDNA in the *cdc13-1* strain and the *cdc13-1exo1* $\Delta$  strain reflects the total activity of Exo1. Since experimental data show that this difference is larger than the amount of ssDNA generated in the *cdc13-1rad24* $\Delta$  strain (Zubko et al., 2004), we suggest that there is also some additional Rad24-independent activation of Exo1 and so have included this in the model. Note that our model does not distinguish between different regions of the telomeres and that the model output represents the total amount of single stranded DNA for all telomeres. To examine the effects of nuclease activity at different regions of the telomere, we would need to modify the model to include a separate species for each telomere and separate reactions for different parts of the telomere.

We also looked at the variability of the amount of single-stranded DNA produced over repeated simulations. We found that the variation from run to run was very small and even with ten simulations, the upper and lower 95% confidence interval for the mean was always within 2% of the mean. Therefore it was not necessary to carry out many repeated simulations.

### **3.2.3. Extending the model to include cell death**

When *cdc13-1rad9* $\Delta$  cells are cultured at the restrictive temperature, it has been found that despite the lack of Rad9, which is required to activate the checkpoint pathway, these cells only divide for a few hours and then die (Zubko et al., 2004). The death of cells is due to the large amounts of single-stranded DNA generated in these mutants. Therefore we modified our model to allow for the possibility of cell death if the total ssDNA for the cell reached a critical threshold of 20kb. There is currently no data on

the amount of ssDNA required to trigger cell death but it has been observed that there is about 15kb of ssDNA present in *cdc13-1exo1Δ* strains (Zubko et al., 2004). So assumed that the threshold must be greater than this and initially chose 20kb. The results for this model are in figure 8 and the model now predicts that the *cdc13-1rad9Δ* cells do not divide since the critical threshold of ssDNA for cell death is reached before it is time to divide (see figure 9a). Therefore we increased the critical threshold for cell death to 120kb and this allows the *cdc13-1rad9Δ* cells to divide two to three times before cell death (see figure 9b). These results agree much better with the experimental data, since the *cdc13-1rad9Δ exo1Δ* cells are able to form larger micro-colonies than both *cdc13-1rad9Δ* cells and *cdc13-1 exo1Δ* cells (see figure 6). However, with this increased threshold, the model predicts that *cdc13-1rad9Δ exo1Δ* cells are able to keep dividing as in the absence of Exo1, the rate of single-strand production is lower and since these cells are dividing, ssDNA can be removed during S phase. This accounts for the zig-zagging line in figure 9a. Since the rate of ssDNA removal depends on the level of ssDNA, there comes a point at which there is a balance between rate of generation and rate of removal of DNA. For the *cdc13-1rad9Δ exo1Δ* cells, this balance occurs somewhere between 60 and 80kb. This suggests that the threshold for cell death might not be as high as 120kb but somewhere in the region of 60 to 80kb. Therefore we did further simulations with a critical threshold of 70kb. In this case, the model predicts that *cdc13-1rad9Δ exo1Δ* cells divide 6-7 times, *cdc13-1exo1Δ* cells divide 3-5 times, *cdc13-1rad9Δ* cells divide just once and *cdc13-1* cells do not divide at all (data not shown).

Simulations were also carried out for *rad53Δ* and *mec1Δ* mutant strains. We found lower rates of ssDNA production in both *cdc13-1rad53Δexo1Δ* and *cdc13-*

*Imec1Δexo1Δ* strains than in *cdc13-1rad9Δexo1Δ* strains which agrees with experimental data (Jia et al., 2004). This ssDNA was the result of ExoX activity, which was not completely inhibited by Rad9. Our models predicted that the rate of ssDNA production was less than 1kb per hour on average for both strains (data not shown).

Table 4 summarises all of the knockout experiments performed and compares the model predictions with the experimental data. Where agreement is not close, a suggestion for modifying the model has been made.

### **3.3. Deterministic versus stochastic simulation**

We also used a deterministic simulator to run the model to examine whether any parts of the model could be successfully modelled using an ODE framework. We found that the generation of ssDNA could be modelled in this way, and the output for the amount of ssDNA is very similar using either a deterministic or stochastic simulator. This is because the variation for the amount of ssDNA for a number of stochastic simulations was small and typically large numbers were involved. However, information was lost for other parts of the model when using a deterministic simulator. For example, in the wild type model the deterministic output for the number of capped and uncapped telomeres gave a steady state of 63.85 and 0.15 respectively which reflects the average number of capped and uncapped telomeres at any point in time whereas output from the stochastic simulator show the exact numbers of capped and uncapped telomeres at any time point. Similarly, the number of divisions obtained by *cdc13-1* mutant strains in a stochastic simulation were generally low integers and showed some variability, whereas the deterministic output could only show the average value.

The advantage of using deterministic models is the greater speed of simulation and so it is worth considering using a hybrid approach where parts of the model are simulated using a deterministic simulator and other parts (for example, low-copy number species) are simulated with a stochastic simulator. There are also hybrid simulators being developed which combine exact stochastic with approximate stochastic algorithms. Further details of hybrid simulation can be found in Kiehl et al. (2004) and Wilkinson (2006).

#### **4. Discussion**

We have developed a mathematical model of the yeast checkpoint response which has been successfully used to test ideas about the checkpoint response to telomere uncapping in budding yeast. The model was modified and used to predict the behaviour of *cdc13-1* cells at the restrictive temperature and in addition we carried out simulations where one or more genes were deleted. We compared simulation output to experimental data of the amount of single-stranded DNA generated over time and the number of cell divisions obtained for the different mutant strains. Generally we found good agreement with our model predictions and the schema in figure 1. We found that it was necessary to include cell death in the model and that the model output depends on the assumption made about the critical threshold of single-stranded DNA for cell death. This has been useful to discover and suggests further experimental work is needed to determine this threshold. To explain the experimental observation that *cdc13-1exo1Δ* initially stop dividing and then escape from cell cycle arrest, it will be necessary to extend the model to include the mechanism of adaptation (see below).

The models have been kept as simple as possible while retaining enough biological realism and provide the starting point for further investigation. They were encoded in SBML, so that they can easily be extended at any point in the network. For example, it is a fairly easy task to add in further proteins that are involved in the network such as the MRX complex (Mre11, Rad50, Xrs2) which may be involved in processing telomeric ends and in telomere capping (Larrivee et al., 2004; Foster et al., 2006). Another protein complex, important at telomeres, is the Yku70/Yku80 heterodimer which has a similar role to Cdc13 in binding telomere ends and protecting them from repair and checkpoint pathways (Maringele & Lydall, 2002). An important kinase which we have not yet included in the model is the Tel1 kinase. Takata et al. (2004) show that Tel1 and Mec1 are recruited reciprocally to telomeres during the cell cycle. Tel1 is recruited to telomeres with a repressive structure and is needed to prevent telomeres from fusing through non-homologous end joining in collaboration with telomerase. Mec1 associates preferentially with shortened telomeres during replication. Our model could be modified to investigate this process.

It might also be desirable to add in further details about some of the proteins that are already in the model. For example, Rad9 functions as a 859 kDa complex in undamaged cells but undergoes conformational change in the presence of DNA damage (Gilbert et al., 2001). This change involves loss of mass and hyperphosphorylation and requires the essential chaperones Ssa1 and Ssa2 (Gilbert et al., 2003). Another example is Mec1, which not only is recruited to damaged DNA but resides at the telomeres even in the absence of damage (Takata et al., 2004). This might affect the kinetics of RPA recruitment to single-stranded DNA and so requires further investigation. Interestingly, a recent study shows that the cell cycle kinase

Cdk1 is required for the recruitment of single-stranded DNA-binding complex, RPA and that it is also involved in degradation which occurs at double-stranded DNA breaks (Ira et al., 2004). There is no direct evidence that it is involved in degradation of single-stranded DNA at telomeres but it would be interesting to see how adding the requirement for Cdk1 to allow RPA binding affects the model predictions.

Further detail of the telomere end protection pathway could also be incorporated into the model. For example, a recent study by Verdun et al. (2005) found that telomeres are unprotected during the G2 phase of the cell cycle and that a localised DNA damage response at telomeres after replication is essential for recruiting the processing machinery that promotes formation of a chromosome end protection complex. Since our model incorporates the cell cycle, it would be fairly straight forward to add this extra detail to the model.

A less straight forward but by no means impossible task is to replace the pool of telomeres with individual telomeres to allow the investigation of telomere dynamics. The easiest way to do this would be to have an array or a set of telomere species in the model. Currently SBML does not support models with arrays or sets but proposals have been put forward to incorporate this feature into SBML Level 3, (see [www.sbml.org](http://www.sbml.org)). The model could then be used to investigate the action of telomerase and the possibility that either abrupt shortening or lengthening may cause cell cycle arrest (Ijpma & Greider, 2003; Viscardi et al., 2003). To examine the effects of nuclease activity at different regions of the telomere (Zubko et al., 2004), we would need additionally to add separate reactions for different parts of the telomere and keep track of the amount of single stranded DNA acquired in the different regions. This

would be very interesting to do and the model could then be used to test the hypotheses that different nucleases are important at different regions of the telomeres (Zubko et al., 2004).

We could also modify our model so that it is possible to carry out simulations which involve changing the temperature of *cdc13-1* mutant strains. A simple way to do this is to add two variables to the model to represent the permissive and restrictive temperature, say Temp23 and Temp36. At the permissive temperature, Temp23 and Temp36 are set to one and zero respectively and at the restrictive temperature, the settings are reversed. The addition of Temp23 to the kinetic law of the capping reaction would ensure that this reaction could only proceed at the permissive temperature (if Temp23=0, then the rate of the reaction would also be zero and so unable to take place). The temperature could be switched at certain time points during the course of the simulation to mimic the experimental procedure of moving cells from the permissive temperature to the restrictive temperature and vice versa.

Experimental data shows that the function of *cdc13-1* is not totally disrupted at 36°C and that there is a negative correlation between function and increasing temperature.

We could model this scenario by having a species in the model to represent the temperature, say *Temp*, and to choose a kinetic law so that the rate of the capping reaction depends on the value of *Temp*. The value of *Temp* could be changed at different time points during the simulation to mimic the experimental procedure of switching temperatures.

The cells for *cdc13-1exo1Δ* strain are larger than in the *cdc13-1rad9Δ* strain which indicates that cells initially arrest and then eventually escape this arrest and divide an

average of eight times before cell death takes place (figure 6 ; Zubko et al., 2004). Our model predicts that the *cdc13-Ixo1Δ* strain divide four or five times and then arrest. Therefore it is desirable to add the possibility of escape from cell arrest into the model. It is known that escape (also known as adaptation) from cell arrest occurs even though the damage and the signal for damage persists and that the time for escape is about 8-15 hours (Gardner et al., 1999; Pellicioli et al., 2001; Toczyski et al., 1997). Studies have shown that escape requires the proteins Cdc5 and casein kinase II (Toczyski et al., 1997) and that Rad53 kinase activity and Chk1 phosphorylation disappear at the time that cells escape arrest provided functional Cdc5 is present (Pellicioli et al., 2001). Cdc5 is a target of Rad53, and phosphorylation of Cdc5 is required for the completion of anaphase (Sanchez et al., 1999). Pellicioli et al. (2001) suggest that Cdc5 acts in a feedback loop to turn off the checkpoint kinase cascade but at present we do not know the exact mechanism of how this is achieved. Trying to model this scenario would help to clarify the details of this pathway.

The models in this paper have followed the fate of one individual cell. It would be interesting to extend the models to follow an entire colony. This would be much more computer intensive to do but should become easier in future as computing power continues to increase. The addition of arrays or sets into SBML would also make it much easier to code population-based models.

Finally the models developed in this paper were motivated by hypotheses put forward as a result of experimental work. Our models do not preclude the possibility that other hypotheses may also be able to explain the experimental results. Therefore we

encourage the interested reader to either make their own modifications to the models or to send us their suggestions so that other ideas can be tested.

## Acknowledgements

This work was funded by BBSRC, MRC, EPSRC, DTI and Unilever plc. DL is also funded by The Wellcome Trust. We thank three anonymous referees for their very helpful suggestions.

## References

- Blankley, R. T. & Lydall, D. 2004. A domain of Rad9 specifically required for activation of Chk1 in budding yeast. *Journal of Cell Science*, **117**, 601-608.
- Foster, S.S., Zubko, M.K., Guillard, S. & Lydall, D. 2006. MRX protects telomeric DNA at uncapped telomeres of budding yeast *cdc13-1* mutants. *DNA Repair* (in press).
- Gardner, R., Putnam, C. W. & Weinert, T. 1999. RAD53, DUN1 and PDS1 define two parallel G(2)/M checkpoint pathways in budding yeast. *Embo Journal*, **18**, 3173-3185.
- Garvik, B., Carson, M. & Hartwell, L. 1995. Single-stranded DNA arising at telomeres in *cdc13* mutants may constitute a specific signal for the Rad9 checkpoint. *Molecular and Cellular Biology*, **15**, 6128-6138.
- Gilbert, C. S., Green, C. M. & Lowndes, N. F. 2001. Budding yeast Rad9 is an ATP-dependent Rad53 activating machine. *Molecular Cell*, **8**, 129-136.
- Gilbert, C. S., van den Bosch, M., Green, C. M., Vialard, J. E., Grenon, M., Erdjument-Bromage, H., Tempst, P. & Lowndes, N. F. 2003. The budding yeast Rad9 checkpoint complex: chaperone proteins are required for its function. *Embo Reports*, **4**, 1-6.
- Gillespie, D. T. 1977. Exact stochastic simulation of coupled chemical reactions. *The Journal of Physical Chemistry*, **31**, 2340-2361.
- Gillespie, C. S., Wilkinson, D. J., Proctor, C. J., Shanley, D. P., Boys, R. J. & Kirkwood, T. B. L. 2006a. Tools for the SBML community. *Bioinformatics* **22**, 628-629.
- Gillespie, C. S., Wilkinson, D. J., Shanley, D. P., Proctor, C. J., Boys, R. J. & Kirkwood, T. B. L. 2006b. BASIS: an internet resource for network modelling (submitted to *Journal of Integrative Bioinformatics*)
- Grandin, N., Damon, C. & Charbonneau, M. 2001a. Cdc13 prevents telomere uncapping and Rad50-dependent homologous recombination. *Embo Journal*, **20**, 6127-6139.
- Grandin, N., Damon, C. & Charbonneau, M. 2001b. Ten1 functions in telomere end protection and length regulation in association with Stn1 and Cdc13. *Embo Journal*, **20**, 1173-1183.

- Hucka, M., Finney, A., Sauro, H. M., Bolouri, H., Doyle, J. C. & Kitano, H. 2003. The systems biology markup language (SBML): a medium for representation and exchange of biochemical network models. *Bioinformatics*, **19**, 524-531.
- Huh, W. K., Falvo, J. V., Gerke, L. C., Carroll, A. S., Howson, R. W., Weissman, J. S. & O'Shea, E. K. 2003. Global analysis of protein localization in budding yeast. *Nature*, **425**, 686-691.
- Ijpm, A. S. & Greider, C. W. 2003. Short telomeres induce a DNA damage response in *Saccharomyces cerevisiae*. *Molecular Biology of the Cell*, **14**, 987-1001.
- Jia, X. D., Weinert, T. & Lydall, D. 2004. Mec1 and Rad53 inhibit formation of single-stranded DNA at telomeres of *Saccharomyces cerevisiae* cdc13-1 mutants. *Genetics*, **166**, 753-764.
- Kiehl, T. R., Mattheyses, R. M. & Simmons, M. K. 2004. Hybrid simulation of cellular behavior. *Bioinformatics*, **20**, 316-322.
- Larrivee, M., LeBel, C. & Wellinger, R. J. 2004. The generation of proper constitutive G-tails on yeast telomeres is dependent on the MRX complex. *Genes & Development*, **18**, 1391-1396.
- Le Novère N., Bornstein B., Broicher A., Courtot M., Donizelli M., Dharuri H., Li L., Sauro H., Schilstra M., Shapiro B., Snoep J.L., Hucka M. 2006. BioModels Database: A free, centralized database of curated, published, quantitative kinetic models of biochemical and cellular systems *Nucleic Acids Res.*, **34**: D689-D691
- Lin, Y. C., Hsu, C. L., Shih, J. W. & Lin, J. J. 2001. Specific binding of single-stranded telomeric DNA by Cdc13p of *Saccharomyces cerevisiae*. *Journal of Biological Chemistry*, **276**, 24588-24593.
- Lydall, D. 2003. Hiding at the ends of yeast chromosomes: telomeres, nucleases and checkpoint pathways. *Journal of Cell Science*, **116**, 4057-4065.
- Lydall, D. & Weinert, T. 1995. Yeast checkpoint genes in DNA damage processing: implications for repair and arrest. *Science*, **270**, 1488-1491.
- Majka, J. & Burgers, P. M. J. 2003. Yeast Rad17/Mec3/Cdc1: A sliding clamp for the DNA damage checkpoint. *Proceedings of the National Academy of Sciences of the United States of America*, **100**, 2249-2254.
- Maringele, L. & Lydall, D. 2002. EXO1-dependent single-stranded DNA at telomeres activates subsets of DNA damage and spindle checkpoint pathways in budding yeast yku70 Delta mutants. *Genes & Development*, **16**, 1919-1933.
- Maringele, L. & Lydall, D. 2005. The PAL-mechanism of chromosome maintenance - Causes and consequences. *Cell Cycle*, **4**, 747-751.
- Pelliccioli, A., Lee, S. B., Lucca, C., Foiani, M. & Haber, J. E. 2001. Regulation of *Saccharomyces* Rad53 checkpoint kinase during adaptation from DNA damage-induced G2/M arrest. *Molecular Cell*, **7**, 293-300.
- Sanchez, Y., Bachant, J., Wang, H., Hu, F. H., Liu, D., Tetzlaff, M. & Elledge, S. J. 1999. Control of the DNA damage checkpoint by Chk1 and Rad53 protein kinases through distinct mechanisms. *Science*, **286**, 1166-1171.
- Schwartz, M. F., Duong, J. K., Sun, Z., Morrow, J. S., Pradhan, D. & Stern, D. F. 2002. Rad9 phosphorylation sites couple Rad53 to the *Saccharomyces cerevisiae* DNA damage checkpoint. *Molecular Cell*, **9**, 1055-1065.
- Shapiro, B. E., Hucka, M., Finney, A. & Doyle, J. 2004. MathSBML: a package for manipulating SBML-based biological models. *Bioinformatics*, **20**, 2829-2831.
- Takata, H., Kanoh, Y., Gunge, N., Shirahige, K. & Matsuura, A. 2004. Reciprocal association of the budding yeast ATM-related proteins Tel1 and Mec1 with telomeres in vivo. *Molecular Cell*, **14**, 515-522.

- Toczyski, D. P., Galgoczy, D. J. & Hartwell, L. H. 1997. CDC5 and CKII control adaptation to the yeast DNA damage checkpoint. *Cell*, **90**, 1097-1106.
- Vaze, M. B., Pelliccioli, A., Lee, S. E., Ira, G., Liberi, G., Arbel-Eden, A., Foiani, M. & Haber, J. E. 2002. Recovery from checkpoint-mediated arrest after repair of a double-strand break requires Srs2 helicase. *Molecular Cell*, **10**, 373-385.
- Verdun, R. E., Crabbe, L., Haggblom, C. & Karlseder, J. 2005. Functional human telomeres are recognized as DNA damage in G2 of the cell cycle. *Molecular Cell*, **20**, 551-561.
- Viscardi, V., Baroni, E., Romano, M., Lucchini, G. & Longhese, M. P. 2003. Sudden telomere lengthening triggers a Rad53-dependent checkpoint in *Saccharomyces cerevisiae*. *Molecular Biology of the Cell*, **14**, 3126-3143.
- Weinert, T. A. & Hartwell, L. H. 1988. The Rad9 gene controls the cell cycle response to DNA damage in *Saccharomyces cerevisiae*. *Science*, **241**, 317-322.
- Wilkinson, D. J. 2006. *Stochastic Modelling for Systems Biology*. Chapman & Hall/CRC Press.
- Zou, L. & Elledge, S. J. 2003. Sensing DNA damage through ATRIP recognition of RPA-ssDNA complexes. *Science*, **300**, 1542-1548.
- Zubko, M. K., Guillard, S. & Lydall, D. 2004. Exo1 and Rad24 differentially regulate generation of ssDNA at telomeres of *Saccharomyces cerevisiae* cdc13-1 mutants. *Genetics*, **168**, 103-115.

## Appendix 1 Modelling the cell cycle

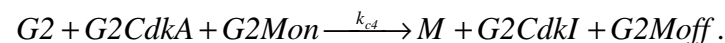
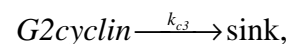
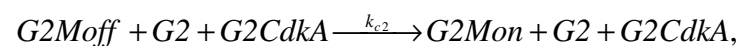
We model the cell cycle by having a species for each of its stages: G1, S, G2, M.

Initially  $G1=1$ , and  $S=G2=M=0$  which means that the cell is in G1 phase. When the cell goes into S phase,  $G1=0$ ,  $S=1$  and so on.

Each phase of the cycle is governed by the growth of a cyclin which must reach a sufficient level before it will bind and activate a protein kinase Cdk. When the Cdk is activated, it signals for the transcription of genes necessary for the transition into the next stage of the cell cycle. When these genes have been transcribed, the cycle can proceed to the next stage. Cyclins are continually degraded but only synthesised during the phase to which they relate. This can be modelled by a set of biochemical reactions and an event which triggers the activation of the Cdk when the cyclin reaches a threshold level. The reactions and event for the G2 to M phase transition are listed below (all the other reactions are easily written down by replacing G2 with M and M with G1 to get the reactions for the M to G1 transition and so on).



If  $G2cyclin > 100$ , then  $G2CdkA = 1, G2CdkI = 0$ ,



$G2CdkI$  represents the inactive kinase and  $G2CdkA$  represent the active form. The first line is the reaction for the synthesis of the G2 cyclin; the second line gives the event which triggers activation of the G2 Cdk; the third line is the reaction for the transcription of genes required for G2 to M phase transition; the fourth line is the reaction for cyclin degradation and the last line is the reaction which results in the transition from G2 to M phase. The parameter values chosen were  $k_{c1}=0.16$ ,  $k_{c2}=0.01$ ,

$k_{c3}=0.0012$  and  $k_{c4}=0.01$ . With these values, each phase lasts about 20 minutes.

Initially all the Cdks are in their inactive state ( $G2CdkI=1$ ,  $G2CdkA=0$ , etc.) , all cell cycle genes are off ( $G2Moff=1$ ,  $G2Mon=0$ , etc.) and the level of each cyclin is zero.

To keep track of the number of cell divisions made by an individual cell, a dummy species called *budscar* was introduced which increased by one every time the cell cycle progressed from the M phase to G1. This was represented by the following reaction:



The rate law for this equation is  $k_{c4}[\#M][\#MG1on][\#MCdkA]$  and since the species M, MG1on and MCdkA can only take the value one or zero, the reaction can only proceed when all of M, MG1on and MCdkA are equal to one.

A complete list of the species used in modelling the cell cycle, the initial amounts, the systematic names for the genes, and database terms are given in table A1. A complete list of reactions and events are given in tables A2 and A3 respectively and figA1 shows the complete network for the cell cycle model.

**Table 1 Initial conditions for wild type model**

Species	Description	Sytematic name (for genes) <sup>a</sup>	Database term <sup>b</sup>	Initial value <sup>c</sup> (no. of molecules)
Ctelo	Capped telomere	N/A <sup>d</sup>	GO:0000781	64
Utelo	Uncapped telomere	N/A	GO:0000781	0
Rad17Utelo	Uncapped telomere bound by Rad17	N/A	GO:0000781	0
Cdc13	Cdc13 protein complex	YDL220C	S000002379	300
Rad17	Rad17 protein complex	YOR368W	S000005895	70
Rad24	Rad24 protein complex	YER173W	S000000975	70
RPA	Replication protein A	YAR007C, YNL312W, YJL173C	GO:0005662	4000
Mec1	Mec1/Ddc2 complex	YBR136W, YDR499W	S000000340 S000002907	4000
ssDNA	Single-stranded DNA (10 nt)	N/A	N/A	0
RPAssDNA	ssDNA bound by RPA	N/A	N/A	0
Mec1RPAssDNA	RPAssDNA bound by Mec1 complex	N/A	N/A	0
ExoXI	Inactive ExoX	unidentified	N/A	70
ExoXA	Active ExoX	unidentified	N/A	0
ExoII	Inactive Exo1	YOR033C	S000005559	670
Exo1A	Active Exo1	YOR033C	S000005559	0
Rad9I	Inactive Rad9	YDR217C	S000002625	20
Rad9A	Active Rad9	YDR217C	S000002625	0
Rad53I	Inactive Rad53	YPL153C	S000006074	6900
Rad53A	Active Rad53	YPL153C	S000006074	0
Chk1I	Inactive Chk1	YBR274W	S000000478	60
Chk1A	Active Chk1	YBR274W	S000000478	0
Dun1I	Inactive Dun1	YDL101C	S000002259	3000
Dun1A	Active Dun1	YDL101C	S000002259	0
ATP	Adenosine triphosphate	N/A	CHEBI:15422	10000
ADP	Adenosine diphosphate	N/A	CHEBI:16761	1000
recovery	dummy species	N/A	N/A	0
sink	dummy species	N/A	N/A	0

<sup>a</sup>Sytematic names (or ORF-name) corresponds to stretch of DNA of the sequenced gene, <sup>b</sup>Database terms starting with: (i) GO, are taken from the Gene Ontology database ([www.geneontology.org](http://www.geneontology.org)); (ii) S, are taken from the Saccharomyces Genome Database ([www.yeastgenome.org](http://www.yeastgenome.org)); (iii) CHEBI, are taken from the Chemical Entities of Biological Interest database ([www.ebi.ac.uk/chebi/](http://www.ebi.ac.uk/chebi/)). <sup>c</sup>Initial amounts of proteins are taken from the yeast GFP fusion database, where available (<http://yeastgfp.ucsf.edu>). <sup>d</sup>N/A= not applicable

**Table 2: Reactions for wild type model**

Reaction	Kinetic Rate Law	Reactants	Products	Parameter	Value <sup>a</sup>
Capping	$k_1[\text{Utelo}][\text{Cdc13}]$	Utelo, Cdc13	Ctelo	$k_1$	$5.0 \times 10^{-4} \text{ mol}^{-1}\text{s}^{-1}$
Uncapping	$k_2[\text{Ctelo}]$	Ctelo	Utelo, Cdc13	$k_2$	$3.85 \times 10^{-4} \text{ s}^{-1}$
Rad17 binding	$\frac{k_3[\text{Utelo}][\text{Rad17}][\text{Rad24}][\text{ATP}]}{5000+[\text{ATP}]}$	Utelo, Rad17, Rad24, ATP	Rad17Utelo, Rad24, ADP	$k_3$	$1.5 \times 10^{-8} \text{ mol}^{-2}\text{s}^{-1}$
ExoX activation	$k_4[\text{ExoXI}][\text{Rad17Utelo}]$	ExoXI, Rad17Utelo	ExoXA, Rad17Utelo	$k_4$	$0.01 \text{ mol}^{-1}\text{s}^{-1}$
ExoX activity	$k_5[\text{Rad17Utelo}][\text{ExoXA}]$	Rad17Utelo, ExoXA	Rad17Utelo, ExoXA, ssDNA	$k_5$	$3.0 \times 10^{-4} \text{ mol}^{-1}\text{s}^{-1}$
Exo1 activation	$k_{6a}[\text{Exo1I}]$	Exo1I	Exo1A	$k_{6a}$	$5.0 \times 10^{-5} \text{ s}^{-1}$
Exo1 Rad24-dep. activation	$k_{6b}[\text{Exo1I}][\text{Rad24}]$	Exo1I, Rad24	Exo1A, Rad24	$k_{6b}$	$5.0 \times 10^{-4} \text{ mol}^{-1}\text{s}^{-1}$
Rad17-indep. Exo1 activity	$k_{7a}[\text{Utelo}][\text{Exo1A}]$	Utelo, Exo1A	Utelo, Exo1A, ssDNA	$k_{7a}$	$3.0 \times 10^{-5} \text{ mol}^{-1}\text{s}^{-1}$
Rad17-dep. Exo1 activity	$k_{7b}[\text{Rad17Utelo}][\text{Exo1A}]$	Rad17Utelo, Exo1A	Rad17Utelo, Exo1A, ssDNA	$k_{7b}$	$3.0 \times 10^{-5} \text{ mol}^{-1}\text{s}^{-1}$
RPA binding 1	$k_{8a}[\text{ssDNA}][\text{RPA}]$	ssDNA, RPA	RPAssDNA1	$k_{8a}$	$0.001 \text{ mol}^{-1}\text{s}^{-1}$
RPA binding 2	$k_{8b}[\text{ssDNA}][\text{RPAssDNA1}]$	ssDNA, RPAssDNA1	RPAssDNA2	$k_{8b}$	$100.0 \text{ mol}^{-1}\text{s}^{-1}$
RPA binding	$k_{8c}[\text{ssDNA}][\text{RPAssDNA2}]$	ssDNA, RPAssDNA2	RPAssDNA	$k_{8c}$	$100.0 \text{ mol}^{-1}\text{s}^{-1}$
Mec1 binding	$k_{8d}[\text{RPAssDNA}][\text{Mec1}]$	RPAssDNA, Mec1	RPAssDNAMec1	$k_{8d}$	$0.004 \text{ mol}^{-1}\text{s}^{-1}$
Rad9 activation	$k_9[\text{Rad9Kin}][\text{Rad9I}]$	Rad9Kin, Rad9I	Rad9Kin, Rad9A	$k_9$	$100.0 \text{ mol}^{-1}\text{s}^{-1}$
ExoX inhibition	$k_{10a}[\text{Rad9A}][\text{ExoXA}]$	Rad9A, ExoXA	Rad9A, ExoXI	$k_{10a}$	$0.05 \text{ mol}^{-1}\text{s}^{-1}$
ExoX Mec1-ind inhibition	$k_{10b}[\text{Rad9A}][\text{ExoXA}]$	Rad9I, ExoXA	Rad9I, ExoXI	$k_{10b}$	$0.05 \text{ mol}^{-1}\text{s}^{-1}$
Rad53 activation	$k_{11}[\text{Rad9A}][\text{Rad53I}]$	Rad9A, Rad53I	Rad9A, Rad53A	$k_{11}$	$10^5 \text{ mol}^{-1}\text{s}^{-1}$
Chk1 activation	$k_{12}[\text{Rad9A}][\text{Chk1I}]$	Rad9A, Chk1I	Rad9A, Chk1A	$k_{12}$	$1.7 \times 10^{-4} \text{ mol}^{-1}\text{s}^{-1}$
Exo1 inhibition	$k_{13}[\text{Rad53A}][\text{Exo1A}]$	Rad53A, Exo1A	Rad53A, Exo1I	$k_{13}$	$1.0 \text{ mol}^{-1}\text{s}^{-1}$
Dun1 activation	$k_{14}[\text{Rad53A}][\text{Dun1I}]$	Rad53A, Dun1I	Rad53A, Dun1A	$k_{14}$	$3.3 \times 10^{-6} \text{ mol}^{-1}\text{s}^{-1}$
Chk1 cell arrest	$k_{15}[\text{Chk1A}][\text{G2Mon}]$	Chk1A, G2Mon	Chk1A G2Moff	$k_{15}$	$0.2 \text{ mol}^{-1}\text{s}^{-1}$
Dun1 cell arrest	$k_{16}[\text{Dun1A}][\text{G2Mon}]$	Dun1A, G2Mon	Dun1A, G2Moff	$k_{16}$	$0.1 \text{ mol}^{-1}\text{s}^{-1}$
Release of Mec1 and RPA in S phase	$k_{17a}[\text{Mec1RPAssDNA}][\text{S}]$	Mec1RPAssDNA, S	3ssDNA Mec1, RPA, S	$k_{17a}$	$0.05 \text{ mol}^{-1}\text{s}^{-1}$
Release of Mec1 and RPA in G2/M arrest	$k_{17b}[\text{Mec1RPAssDNA}][\text{G2Moff}]$	Mec1RPAssDNA, G2Moff	3ssDNA Mec1, RPA, G2Moff	$k_{17b}$	$0.05 \text{ mol}^{-1}\text{s}^{-1}$
Removal of ssDNA in S phase	$k_{18a}[\text{ssDNA}][\text{S}]$	ssDNA, S	S	$k_{18a}$	$0.001 \text{ mol}^{-1}\text{s}^{-1}$
Removal of ssDNA in G2/M arrest	$k_{18b}[\text{ssDNA}][\text{G2Moff}]$	ssDNA, G2Moff	G2Moff	$k_{18b}$	$1 \times 10^{-5} \text{ mol}^{-1}\text{s}^{-1}$
Recovery	$k_{19}[\text{Rad17Utelo}][\text{Cdc13}][\text{recovery}]$	Rad17Utelo, Cdc13, recovery	Ctelo, Rad17, recovery	$k_{19}$	$0.001 \text{ mol}^{-2}\text{s}^{-1}$

<sup>a</sup>mol=number of molecules

**Table 3 Summary of events used in all models**

<b>Event</b>	<b>Trigger</b>	<b>Species affected</b>	<b>Parameters affected</b>	<b>Reactions affected</b>
Rad9 kinase activation	Mec1RPAssDNA>800	Rad9Kin	None	Rad9 activation
ssDNA removal	Mec1RPAssDNA +RPAssDNA+ssDNA<1	recovery	None	Recovery
G2/M recovery completed	Rad17Utelo==0 && G2==1	G2Moff, G2Mon, recovery, ExoXA, ExoXI, Exo1A, Exo1I, Rad9A, Rad9I, Rad53A, Rad53I, Chk1A, Chk1I, Dun1A, Dun1I	None	All reactions involving ExoX, Exo1, Rad9, Rad53, Chk1, Dun1. Recovery reaction stops
S phase recovery completed	Rad17Utelo==0	recovery	None	Recovery
Cell death <sup>a</sup>	Mec1RPAssDNA +RPAssDNA+ssDNA>2000	None	$k_{alive}$ <sup>b</sup>	All reactions stop

<sup>a</sup> only in models with cell death, <sup>b</sup> $k_{alive}$  is a parameter which is included in all the kinetic rate laws (e.g.  $k_{alive} \times k_2[ Ctelo ]$ ). Initially  $k_{alive}=1$  and so rate laws are unaffected by this parameter. When the critical threshold of total single-stranded DNA is reached  $k_{alive}$  is set to 0, and so all reaction rates are equal to zero.

**Table 4 Summary table of knockout simulations for cdc13-1 strains (model with cell death)**

<b>Gene(s) knocked out</b>	<b>Initial conditions specific for knockout</b>	<b>Behaviour predicted by model</b>	<b>Experimental results</b>	<b>Comparison of predictions with data</b>	<b>Suggested improvement to model (where required)</b>	<b>References</b>
rad9	Rad9I=0	0-1 divisions <sup>a</sup> ~20 kb of ssDNA after 1 hr	3-5 divisions <sup>b</sup> very high levels of ssDNA	model predicts less divisions than observed	increase threshold of ssDNA (see fig 9)	Zubko et al., 2004
exo1	Exo1I=0	1-5 divisions ~3kb of ssDNA after 4 hrs	1-4 divisions low levels of ssDNA	good agreement	add mechanism of adaptation	Zubko et al., 2004
rad9, exo1	Rad9I=0, Exo1I=0	1-4 divisions ~20kb of ssDNA after 6 hrs	2-7 divisions high levels of ssDNA	model predicts less divisions than observed	increase threshold of ssDNA (see fig 9)	Zubko et al., 2004
rad24	Rad24=0	3-5 divisions ~6kb of ssDNA after 6 hrs	0-7 divisions low levels of ssDNA	good agreement	N/A <sup>c</sup>	Zubko et al., 2004
rad24, exo1	Rad24=0, Exo1I=0	no cell arrest no ssDNA	no cell arrest very low levels of ssDNA	good agreement	N/A	Zubko et al., 2004
rad9, rad24	Rad9I=0, Rad24=0	no cell arrest ~6kb after 6 hours	no cell arrest low levels of ssDNA	good agreement	N/A	Zubko et al., 2004
rad9, rad24, exo1	Rad9I=0, Rad24=0, Exo1I=0	no cell arrest no ssDNA	no cell arrest very low levels of ssDNA	good agreement	N/A	Zubko et al., 2004
rad53, exo1	Rad53I=0, Exo1I=0	~3kb of ssDNA after 4 hrs	low levels of ssDNA	good agreement	N/A	Jia et al., 2004
mec1, exo1	Mec1=0, Exo1I=0	~3kb of ssDNA after 4 hrs	low levels of ssDNA	good agreement	N/A	Jia et al., 2004

<sup>a</sup>predicted number of divisions in a 15 hour period, <sup>b</sup>number of divisions per cell in a 15 hour period, estimated from the mean and standard deviation of colony size as given in Zubko et al., (2004), <sup>c</sup>N/A=not applicable.

**Table A1 Identifiers and initial conditions for cell cycle**

Species	Description	Sytematic name <sup>a</sup> (for genes)	Database term <sup>b</sup>	Initial value (number of molecules)
G1	G1 phase	N/A <sup>c</sup>	GO:0051318	1
S	S	N/A	GO:0000084	0
G2	G2	N/A	GO:0051319	0
M	M	N/A	GO:0000279	0
G1cyclin	G1 cyclin	YMR199W	S000004812	0
Scyclin	S cyclin	YPR120C	S000006324	0
G2cyclin	G2 cyclin	YPR119W	S000006323	0
Mcyclin	M cyclin	YGR108W	S000003340	0
G1CdkI	Inactive Cdk	YBR160W	S000000364	0
G1CdkA	Active Cdk	YBR160W	S000000364	0
SCdkI	Inactive Cdk	YBR160W	S000000364	0
SCdkA	Active Cdk	YBR160W	S000000364	0
G2CdkI	Inactive Cdk	YBR160W	S000000364	0
G2CdkA	Active Cdk	YBR160W	S000000364	0
MCdkI	Inactive Cdk	YBR160W	S000000364	0
MCdkA	Active Cdk	YBR160W	S000000364	0
G1Soff	G1toS transition off	N/A	GO:0000082	1
G1Son	G1toS transition on	N/A	GO:0000082	0
SG2off	S to G2 transition off	N/A	GO:0000115	1
SG2on	S to G2 transition on	N/A	GO:0000115	0
G2Moff	G2 to M transition off	N/A	GO:0031572	1
G2Mon	G2 to M transition on	N/A	GO:0000086	0
MG1off	M to G1 transition off	N/A	GO:0000087	1
MG1on	M to G1 transition on	N/A	GO:0000087	0
budscar	scar on membrane for each division	N/A	N/A	0

<sup>a</sup>Sytematic names (or ORF-name) corresponds to stretch of DNA of the sequenced gene, <sup>b</sup>Database terms starting with: (i) GO, are taken from the Gene Ontology database ([www.geneontology.org](http://www.geneontology.org)); (ii) S, are taken from the Saccharomyces Genome Database ([www.yeastgenome.org](http://www.yeastgenome.org)). <sup>c</sup>N/A= not applicable

Table A2 Reactions for the cell cycle

Reaction	Kinetic rate law	Reactants	Products	Parameter	Value <sup>a</sup>
G1 cyclin synthesis	$k_{c1}[G1]$	G1	G1, G1cyclin	$k_{c1}$	$0.16 \text{ s}^{-1}$
S cyclin synthesis	$k_{c1}[S]$	S	S, Scyclin	$k_{c1}$	$0.16 \text{ s}^{-1}$
G2 cyclin synthesis	$k_{c1}[G2]$	G2	G2, G2cyclin	$k_{c1}$	$0.16 \text{ s}^{-1}$
M cyclin synthesis	$k_{c1}[M]$	M	M, Mcyclin	$k_{c1}$	$0.16 \text{ s}^{-1}$
G1 to S genes on	$k_{c2}[G1][G1Soff][G1CdkA]$	G1, G1Soff, G1CdkA	G1, G1Son, G1CdkA	$k_{c2}$	$0.01 \text{ mol}^{-2}\text{s}^{-1}$
S to G2 genes on	$k_{c2}[S][SG2off][SCdkA]$	S, SG2off, SCdkA	S, SG2on, SCdkA	$k_{c2}$	$0.01 \text{ mol}^{-2}\text{s}^{-1}$
G2 to M genes on	$k_{c2}[G2][G2Moff][G2CdkA]$	G2, G2Moff, G2CdkA	G2, G2Mon, G2CdkA	$k_{c2}$	$0.01 \text{ mol}^{-2}\text{s}^{-1}$
M to G1 genes on	$k_{c2}[M][MG1off][MCdkA]$	M, MG1off, MCdkA	M, MG1on, MCdkA	$k_{c2}$	$0.01 \text{ mol}^{-2}\text{s}^{-1}$
G1 cyclin degradation	$k_{c3} [G1cyclin]$	G1cyclin	sink	$k_{c3}$	$0.0012 \text{ s}^{-1}$
S cyclin degradation	$k_{c3} [Scyclin]$	Scyclin	sink	$k_{c3}$	$0.0012 \text{ s}^{-1}$
G2 cyclin degradation	$k_{c3} [G2cyclin]$	G2cyclin	sink	$k_{c3}$	$0.0012 \text{ s}^{-1}$
M cyclin degradation	$k_{c3} [Mcyclin]$	Mcyclin	sink	$k_{c3}$	$0.0012 \text{ s}^{-1}$
G1 to S progression	$k_{c4} [G1][G1CdkA][G1Son]$	G1, G1CdkA, G1Son	S, G1CdkI, G1Soff	$k_{c4}$	$0.01 \text{ mol}^{-2}\text{s}^{-1}$
S to G2 progression	$k_{c4} [S][SCdkA][SG2on]$	S, SCdkA, SG2on	G2, SCdkI, SG2off	$k_{c4}$	$0.01 \text{ mol}^{-2}\text{s}^{-1}$
G2 to M progression	$k_{c4} [G2][G2CdkA][G2Mon]$	G2, G2CdkA, G2Mon	M, G2CdkI, G2Moff	$k_{c4}$	$0.01 \text{ mol}^{-2}\text{s}^{-1}$
M to G1 progression	$k_{c4} [M][MCdkA][MG1on]$	M, MCdkA, MG1on	G1, MCdkI, MG1off, budscar	$k_{c4}$	$0.01 \text{ mol}^{-2}\text{s}^{-1}$

<sup>a</sup>mol=number of molecules

**Table A3 List of events affecting cell cycle**

<b>Event</b>	<b>Trigger</b>	<b>Species affected</b>	<b>Reactions affected</b>
G1Cdk activation	G1cyclin>100	G1CdkA, G1CdkI	G1 to S genes on, G1 to S progression
SCdk activation	Scyclin>100	SCdkA, SCdkI	S to G2 genes on, S to G2 progression
G2Cdk activation	G2cyclin>100	G2CdkA, G2CdkI	G2 to M genes on, G2 to M progression
MCdk activation	Mcyclin>100	MCdkA, MCdkI	M to G1 genes on, M to G1 progression

## Figure Legends

Figure 1. A model for the interaction between checkpoint pathways and nucleases at *cdc13-1* induced damage (Reproduced with permission from Jia et al 2004, Copyright Genetics Society of America.).

Figure 2. Network diagram showing the checkpoint response to uncapped telomeres

(a) Activation of ExoX and Exo1. ExoX requires Rad24 and Rad17 binding for its activation. Exo1 is activated independently of Rad24 and Rad17, although it may also act on telomeres bound by Rad17 and be activated in a Rad24 dependent manner. (b) Binding of single-stranded DNA (ssDNA) by RPA. Each molecule of RPA requires 3 units of ssDNA to bind. (c) Activation of checkpoint response via Rad53/Dun1 pathway. Activation of this pathway leads to inhibition of nuclease activity. Dashed line indicates an event where a threshold level of Mec1RPA<sub>ssDNA</sub> activates a kinase (Rad9Kin) which activates Rad9. (d) Activation of checkpoint response via Chk1 pathway leads to inhibition of ExoX but does not affect Exo1. (e) Recovery can take place during S phase or G2/M arrest after single-stranded DNA has been removed. The dashed line indicates an event. When the level of ssDNA is equal to zero, the dummy species “recovery” is set to one and the recapping reaction can then occur. See section 2.1.6 for more details.

Figure 3. Model predictions of the number of capped telomeres in a wild-type cell when  $k_1 = 3.6 \times 10^{-6}$  or  $k_1 = 0.0005$ . The output is for one simulation over a period of 12 hours.

Figure 4. Model predictions for the kinetics of uncapping in the *cdc13-1* strain at the restrictive temperature (with the default parameters). The output is for one simulation over a period of 12 hours.

Figure 5. Model predictions for the number of divisions obtained in a wild-type cell. The output is for three simulations over a period of 12 hours.

Figure 6. Growth of wild-type and *cdc13-1* mutant strains (reproduced with permission from Zubko et al. 2004, Copyright Genetics Society of America.). Yeast strains were released from G1 arrest and allowed to form microcolonies for 15 hr at 36°C (restrictive temperature) before being photographed at 200x magnification. Cell numbers within microcolonies were estimated from the photographs shown and are indicated along with their standard deviations.

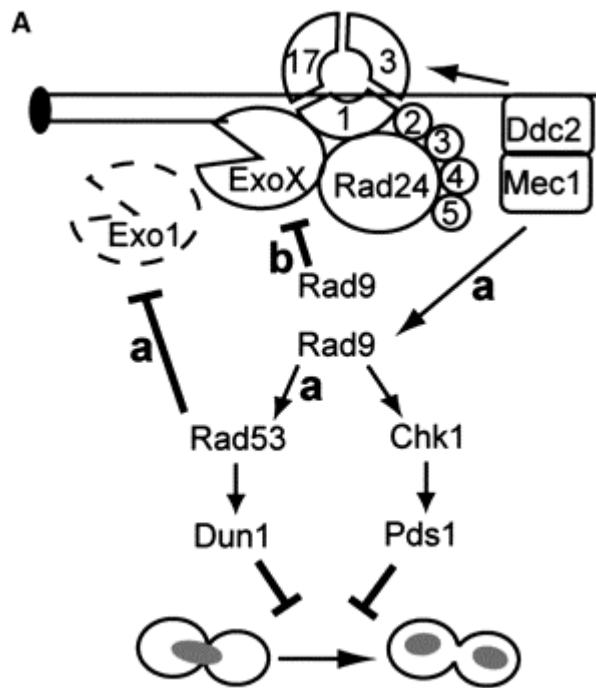
Figure 7. Model predictions for the amount of ssDNA generated in wild-type and *cdc13-1* mutant strains. The output is for one simulation for each strain over a period of 250 minutes.

Figure 8. Model predictions for the number of divisions obtained by wild-type and *cdc13-1* mutant strains if a critical threshold of 20kb ssDNA triggers cell death. The output is for one simulation for each strain over a period of 12 hours.

Figure 9 Model predictions for (a) the amount of ssDNA per cell and (b) the number of cell divisions if a critical threshold of 120kb ssDNA triggers cell death. The output is for one simulation for each strain over a period of 12 hours.

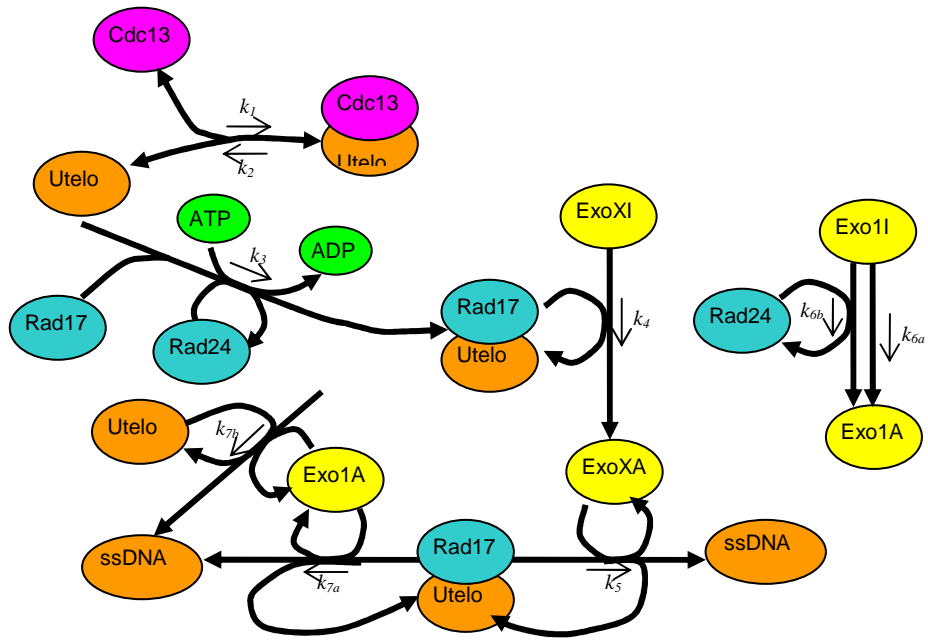
Figure A1 Network diagram of the cell cycle model. G1CdkA and G1CdkI represent the active and inactive G1 Cdk respectively and similarly for the other Cdks. The dashed lines connecting the cyclins to the Cdks indicate events. When a cyclin reaches a level of 100, the respective Cdk is activated.

Figure 1

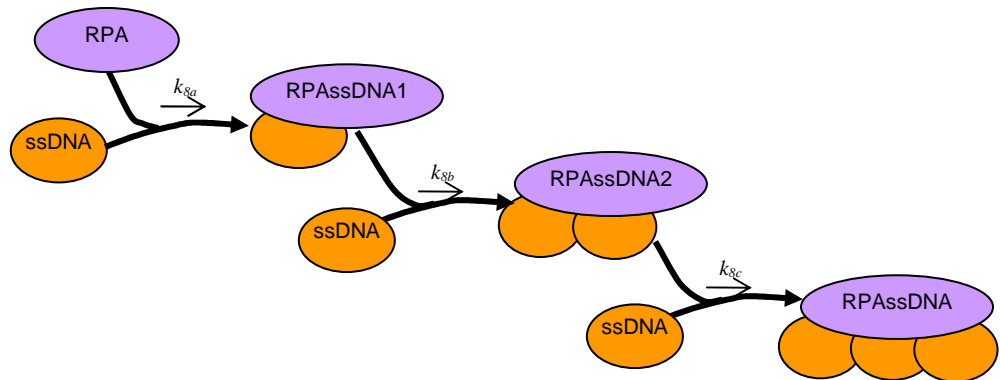


Copyright Genetics Society of America.

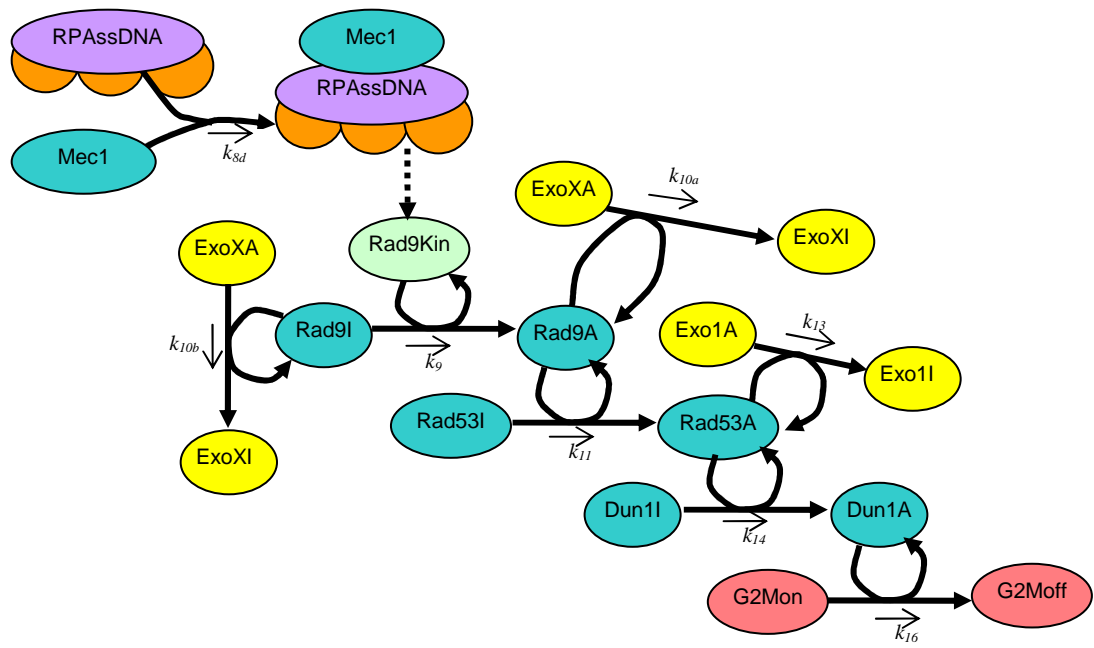
Figure 2  
(a)



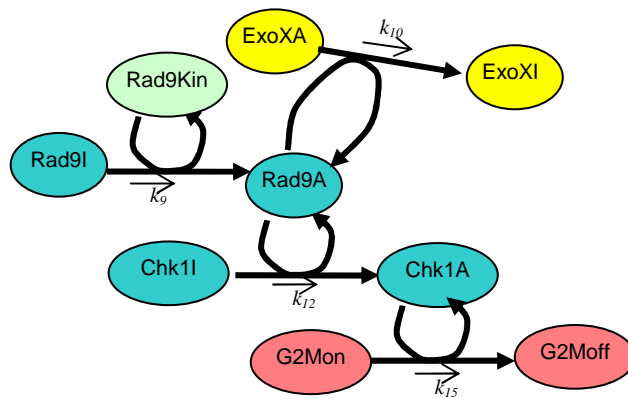
(b)



(c)



(d)



(e)

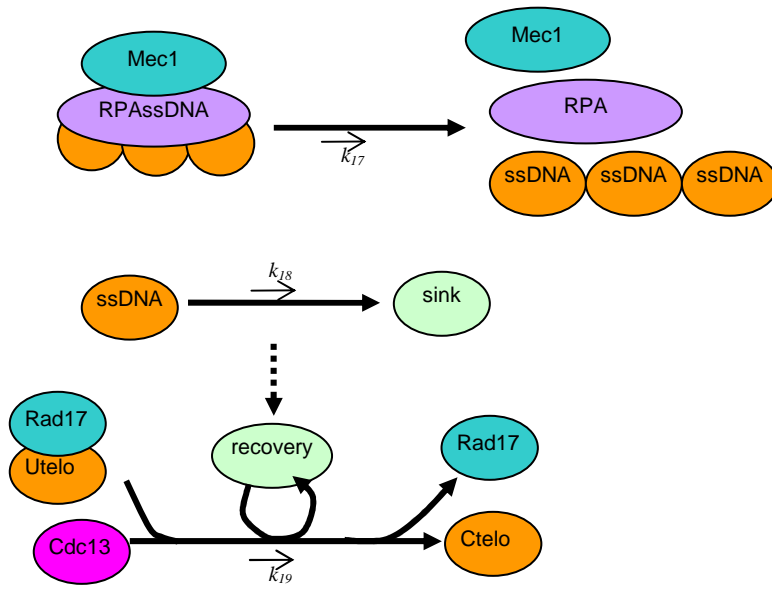


Figure 3

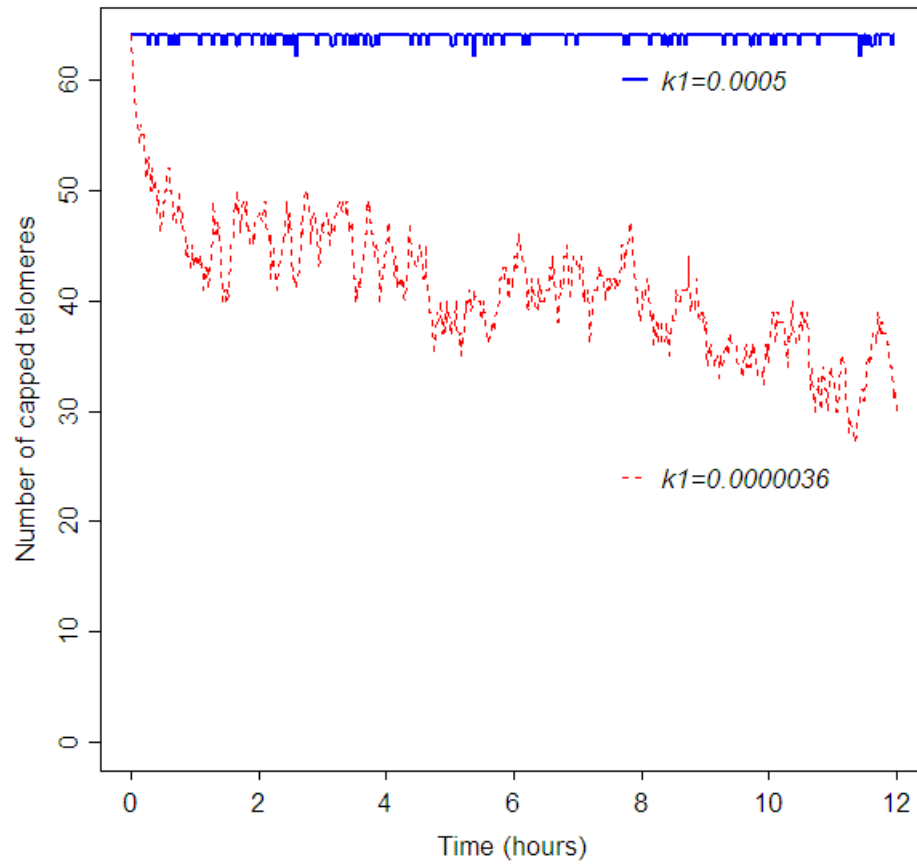


Figure 4

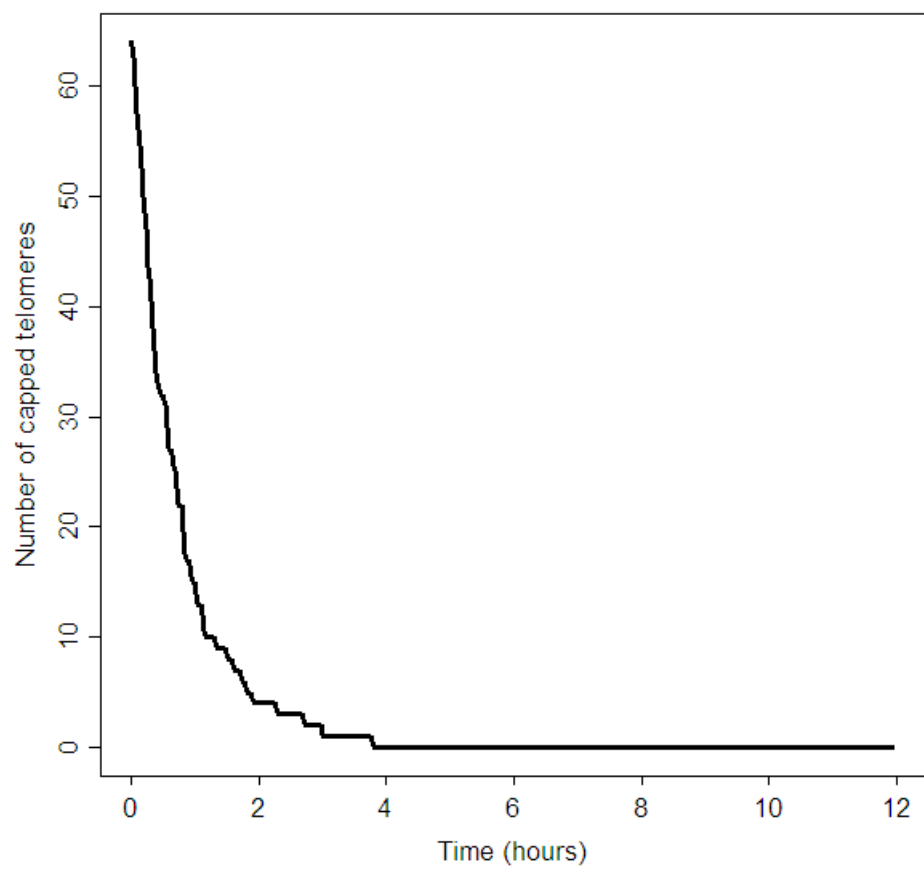


Figure 5

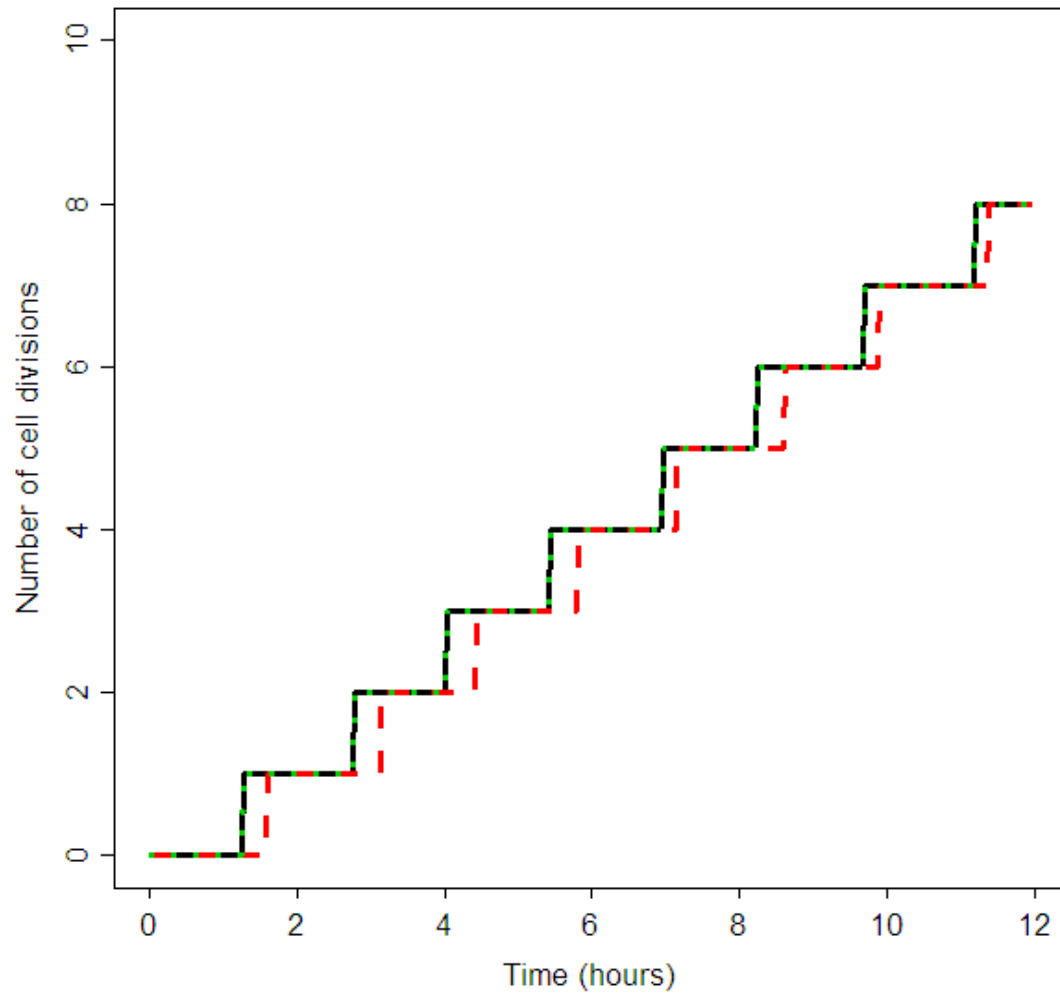
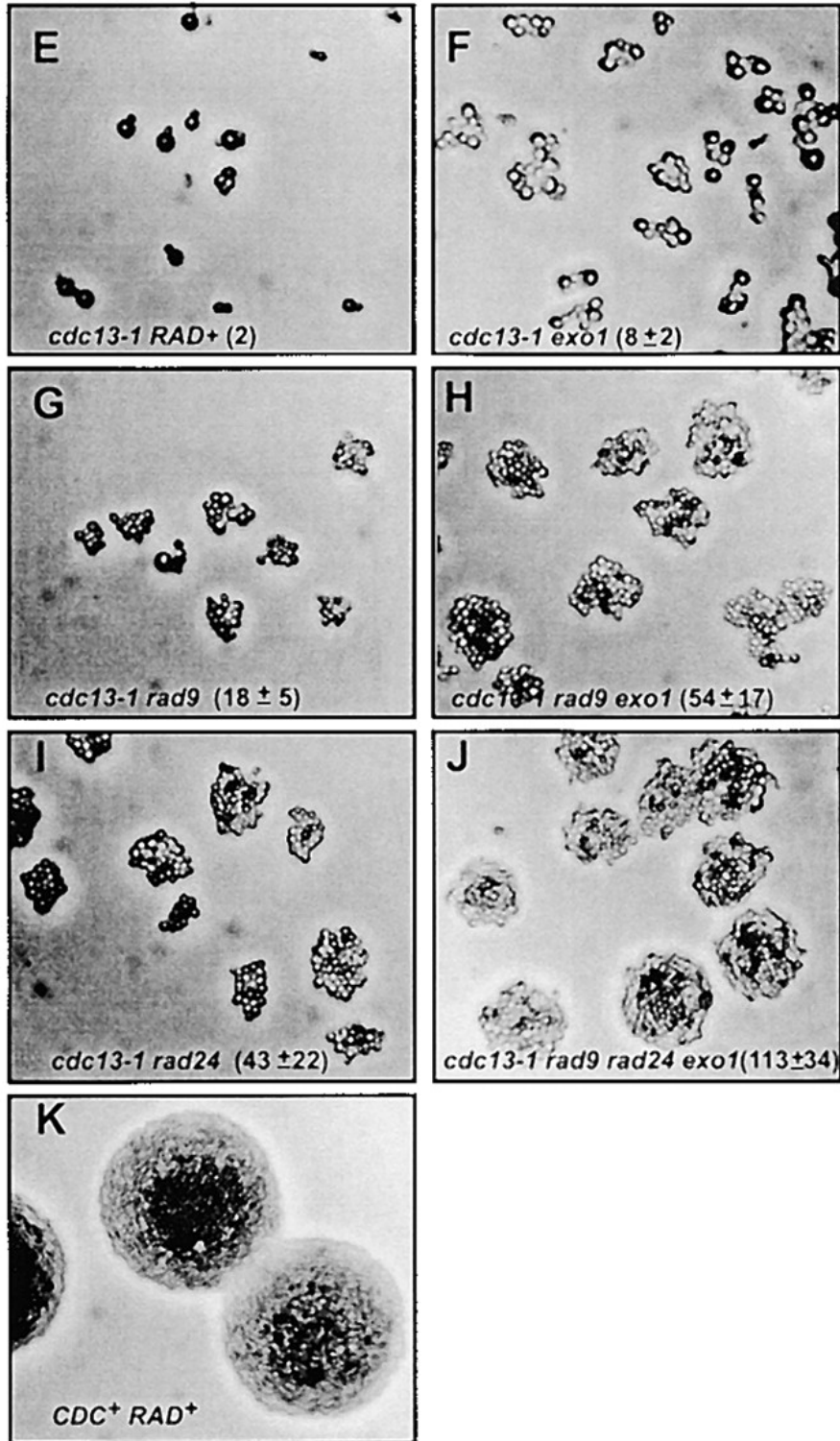


Figure 6



Copyright Genetics Society of America.

Figure 7

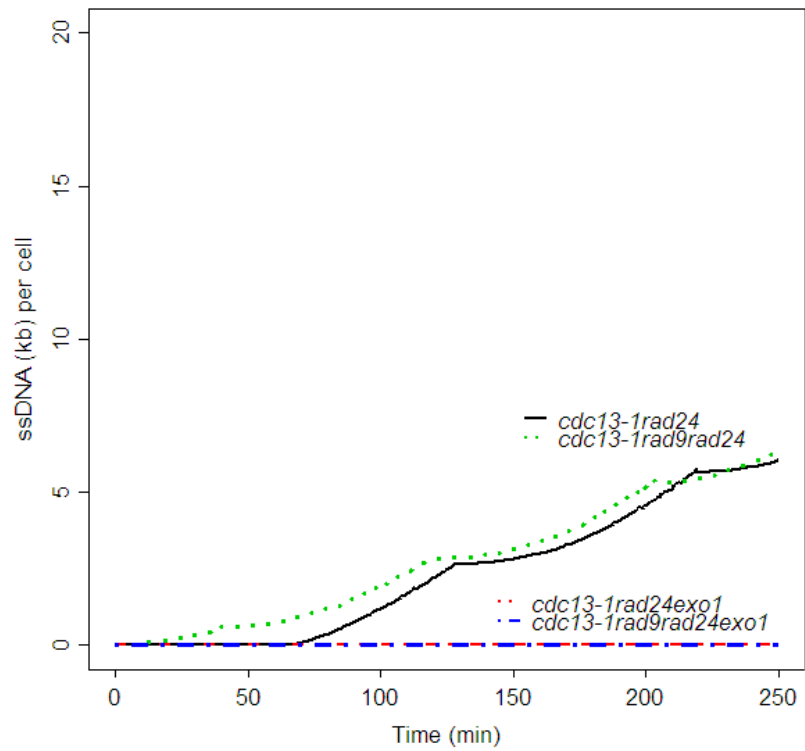
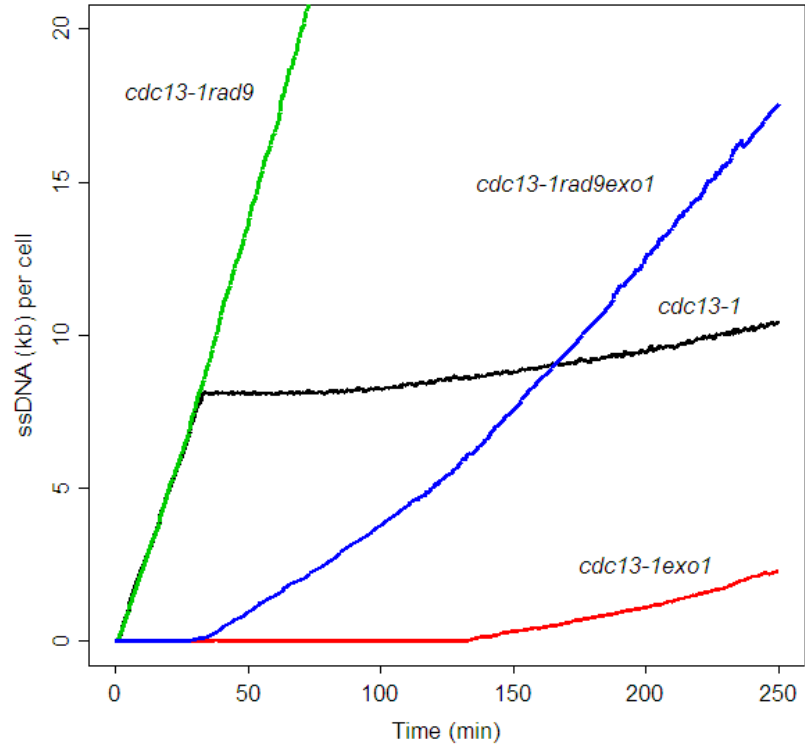


Figure 8

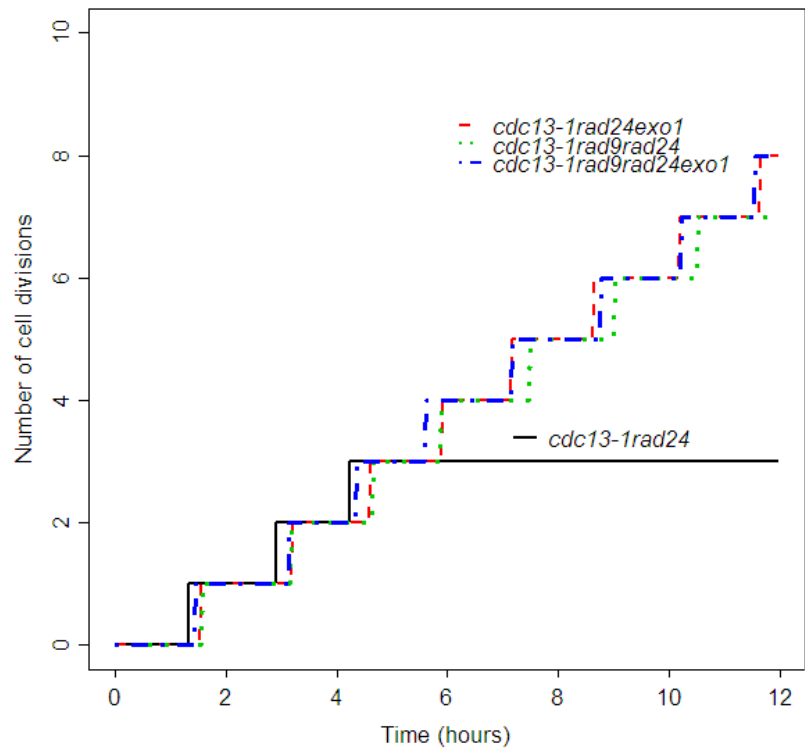
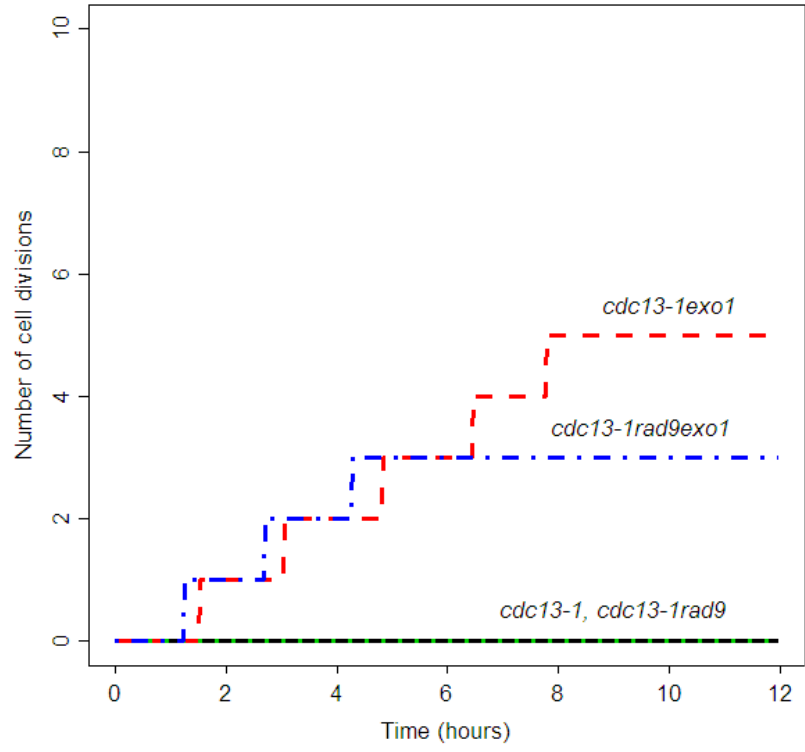
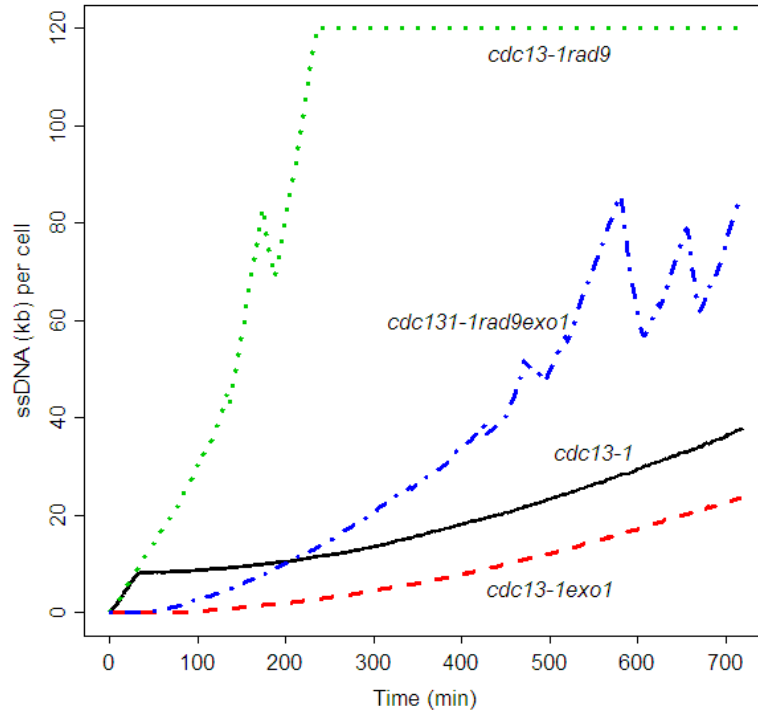


Figure 9

(a)



(b)

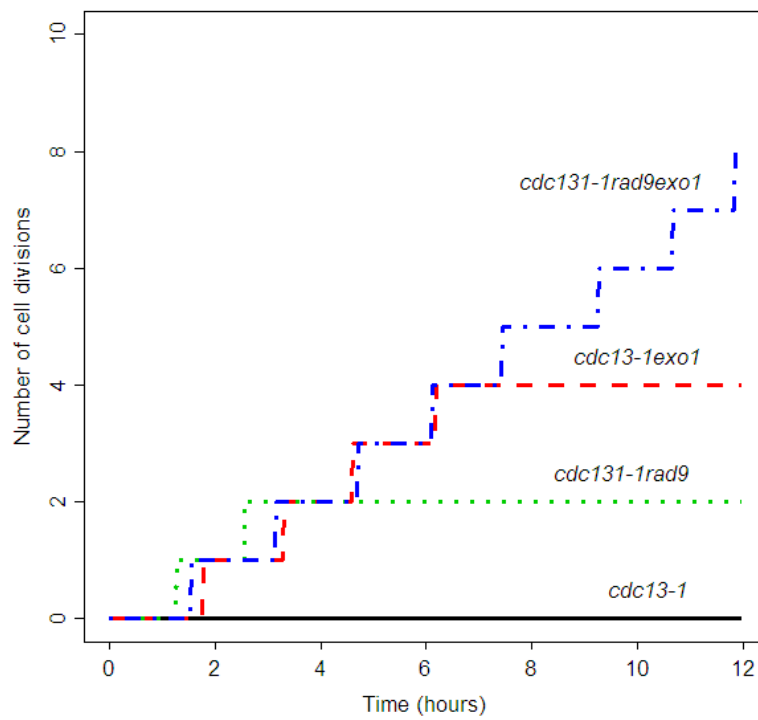


Figure A1

